REVIEW

Check for updates

A review of recent progress in polymeric electrospun nanofiber membranes in addressing safe water global issues

Subrahmanya T. M., [ID] [a] Ahmad Bin Arshad,[b] Po Ting Lin,*[b] Januar Widakdo [ID] [a] Makari H. K., [ID] [c] Hannah Faye M. Austria,[a] Chien-Chieh Hu,[a] Juin-Yih Lai[a] and Wei-Song Hung [ID] *[a]

With rapid advancement in water filtration materials, several efforts have been made to fabricate electrospun nanofiber membranes (ENMs). ENMs play a crucial role in different areas of water treatment due to their several advantageous properties such as high specific surface area, high interconnected porosity, controllable thickness, mechanical robustness, and wettability. In the broad field of water purification, ENMs have shown tremendous potential in terms of permeability, rejection, energy efficiency, resistance to fouling, reusability and mechanical robustness as compared to the traditional phase inversion membranes. Upon various chemical and physical modifications of ENMs, they have exhibited great potential for emerging applications in environment, energy and health sectors. This review firstly presents an overview of the limiting factors influencing the morphology of electrospun nanofibers. Secondly, it presents recent advancements in electrospinning processes, which helps to not only overcome drawbacks associated with the conventional electrospinning but also to produce nanofibers of different morphology and orientation with an increased rate of production. Thirdly, it presents a brief discussion about the recent progress of the ENMs for removal of various pollutants from aqueous system through major areas of membrane separation. Finally, this review concludes with the challenges and future directions in this vast and fast growing area.

[a]Advanced Membrane Materials Research Centre, Graduate Institute of Applied Science and Technology, National Taiwan University of Science and Technology, Taipei, 10607, Taiwan. E-mail: wshung@mail.ntust.edu.tw

[b]Department of Mechanical Engineering, National Taiwan University of Science and Technology, Taipei, 10607, Taiwan. E-mail: potinglin@mail.ntust.edu.tw

[c]Department of Biotechnology, IDSG Government College, Chikkamagaluru, Karnataka, 577102, India

Introduction

The rapid growth in global population, urbanization, and industrialization has led to several complications such as depletion of natural energy resources, environmental pollution causing climate change, and potential health risks including scarcity of food and potable water. Efficient treatment of wastewater and sustainable utilization of renewable energy sources to harvest clean water and energy could be the most promising approach to tackle these issues.[1] In this regard, the ENMs are fascinating materials due to their tuneable versatile properties making them promising materials for water treatment applications. Several techniques have been proposed to produce nanofibers such as template synthesis,[2] self-assembly,[3] solvothermal synthesis, electro hydrodynamic direct writing,[4] centrifugal jet spinning,[5] plasma induced synthesis,[6] solution

blow spinning,[7] CO_2 laser supersonic drawing,[8] and sono-chemical synthesis.[9] Electrospinning is an effective and key technique for enabling continuous production of nanofibers for fabrication of porous materials. The use of electrospun nano-fibers has been proved to be a promising choice not only for filtration materials but also for various other applications such as, environmental remediation, protection sensors in defence and security, optical application, conducting and insulating nanofibers in electrical applications, scaffolds, films and composites in health care, and packaging applications.[10,11] The production of nanofibers by electrospinning was first patented in the year 1934.[12] However, significant progress has been made by Reneker's group after 1990. This invention greatly influenced researchers to study polymer nanofibers for various applications in the broad areas like energy, healthcare and environment. A typical electrospinning instrument has different parts, a high voltage power supply, a metallic spinneret and an electrically earthed metallic collector as shown in Fig. 1. When a high voltage direct current is applied, a drop of a polymer solution suspended at the tip of the spinneret will turn into a conical shaped droplet from its semi sphere shape known as the Taylor cone.[13] When high voltage is applied, the electrostatic repulsive force acting on the surface of the droplet of a polymer solution counteracts the surface tension and forms the Taylor

cone followed by the formation of liquid jet that is deposited onto the collector placed at a specified distance to form nanofibers. The recent tremendous progress in experimental design and upscaling, and vast opportunity for materials choice (polymers, ceramics, functional molecules, carbon and metal/metal oxides) have enabled the production of a wide variety of morphology of nanofibers, such as hollow fibers, core–sheath nanofibers, nanoribbons and nanofibers with various surface topographies (porous, rough surface).[14]

Since fresh water sources are gradually depleting and getting contaminated by verities of pollutants, it is necessary to fabricate membrane materials of high rejection efficiency, flux performance and reusability, to treat wastewater in a simple and cost effective way. These kind of complex issues require the use of electrospun fabricated purification materials such as membranes, absorbents, adsorbents, and scaffolds. From the past few years, many efforts have been made across the world to develop suitable energy efficient ENMs to expel various types of pollutants from aqueous system. The membranes obtained from conventional phase inversion techniques have many disadvantages such as low permeance, fouling propensity, uneven pore size and poor mechanical strength. Nanofiber membranes fabricated *via* electrospinning have been often used as the best substitutes that can outperform conventional membranes due to their high interconnected porosity, tuneable thickness and pore size distribution from few nanometres to several microns, and high surface area for tuning the surface chemistry.[15] Moreover, solvent induced fusion of inter fiber junctions and enhanced crystallinity of nanofibers, impart mechanical robustness to ENMs, and due to high surface area, the surface chemistry of ENMs can be easily and effectively modified. In addition, the recyclable and reusable ENMs of eco-friendly polymers have significantly controlled the negative impact of non-degradable commodity polymer based phase inversion membranes on environment. The present review

firstly aims at understanding the limiting factors of electrospinning influencing the properties of nanofibers on the basis of important morphological investigations reported earlier for various different polymeric nanofibers. Secondly, it introduces an overview of the recent advancements in electrospinning technique and its advantages to produce variety of nanofibers. Thirdly, it provides an overview of use of variety of polymeric ENMs and their efficiency of the expulsion of various pollutants from aqueous system *via* different membrane separation processes, such as microfiltration, desalination (*via* membrane distillation (MD), reverse osmosis (RO), and forward osmosis (FO)), heavy metal removal and oil/water separation. Finally, the review provides a summary and outlook for the future in these vast fields.

Limiting factors and their influence on morphology of nanofibers

Understanding the influence of limiting factors on the properties of electrospun nanofibers is very crucial to fabricate nanofibers with desirable properties. These limiting factors are broadly categorized as solution factors, processing factors, and ambient factors.[16] In these factors, firstly we discuss about the solution factors such as concentration, molecular weight, viscosity, and conductivity, secondly we discuss the processing factors such as flow rate, voltage, and needle tip to collector distance (TCD). Finally, we discuss the influence of temperature and humidity under ambient factors.

Solution factors

In electrospinning, changing the concentration of a polymer solution has significant effect on the transformation of a solution droplet at the needle (spinneret) tip into a charged uniaxial jet. For polymer solutions of very low concentration, under the influence of an applied electric field, the fragmentation of polymer entanglements occurs. As a result, instead of nanofibers micro or nano beads will be formed.[17] If the solution concentration is little higher than the optimum concentration, beaded nanofibers will be formed. If the solution concentration is within an optimum range, the nanofibers without beaded structures will be formed. By tuning the concentration of a polymer solution; viscosity and surface tension of a solution can be optimized, which eventually leads to the formation of smoother nanofibers. Furthermore, if the concentration of a solution is beyond its critical range, polymer solution may clot at the spinneret tip hindering the further flow of a solution. This process is called as clogging. This results in morphological changes in nanofibers such as beaded structures or helix shaped micro ribbons. For instance, Senthil *et al.* studied the influence of concentration on electrospinnability of styrene-acrylonitrile (SAN)–dimethylformamide (DMF) solutions of various concentrations ranging from 8 to 30 wt/v%. They obtained beads at a concentration range of 8–10 wt/v%, and mixture of beads and nanofibers at a concentration range of 12–20 wt/v% and smooth and continuous fibers at 25–30 wt/v% (Fig. 2A).[18] Similar observations were also reported by Hekmati *et al.*[19] and Noorpoor *et al.* for nylon nanofibers.[20] K.P. Matabola
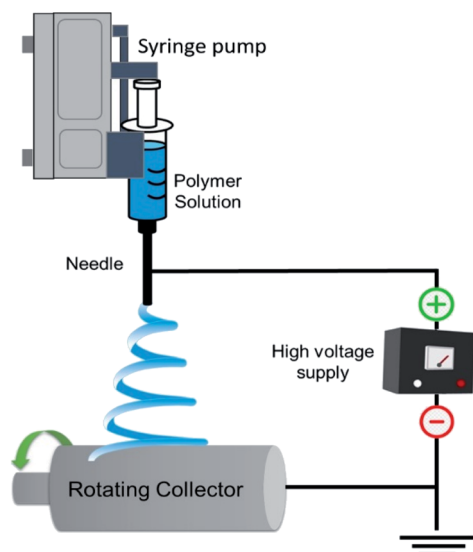

Fig. 1 Schematic diagram showing the different components of a typical electrospinning.

used polyvinylidene fluoride-dimethylacetamide (PVDF-DMAC) solution at different concentrations (22–28 wt%) for electrospinning. They found large bubble like structures at lower concentrations and smooth fibers at higher concentrations with increase of fiber diameter from 98 nm to 397 nm.[21] Similar observation was reported by Hao Shao *et al.* for electrospinning of PVDF/(DMF/acetone) solution.[22] Other than PVDF fibers, the nanofibers of polyurethane (PU),[23] polyacrylonitrile (PAN),[24] polyvinyl alcohol (PVA)[25] and poly(L-lactide),[26] were also found following the similar trend in response to the increase of concentration from lower to higher. Hence, an optimal concentration is necessary to increase the viscosity of a solution which eventually increase the polymer chain entanglements to lead to the formation of smoother beadless nanofibers.

Besides the influence of solution concentration, the effects of viscosity and molecular weight have also been studied for their influence on properties of nanofibers. At higher viscosity of a solution, thickness of the jet increases, leading to the formation of thick nanofibers. For the case of lower viscosity, under the influence of factors such as surface tension and electric field, fragmentation of polymer entanglements occurs. This forms either beads or beaded fibers. When the viscosity of a solution gradually increases towards its optimum range, the morphology of nanofibers turns from beaded shape to spindle shape. Once the viscosity reaches its optimal range, viscoelastic forces prevent the fragmentation of polymer chains and thus results in continuous uniform nanofiber formation. Further increase of viscosity to the level greater than an optimal range (Fig. 2B), wide and flat ribbon like fibers will be formed.[28,29] The molecular weight of a polymer is another crucial factor changing morphological and physical properties of nanofibers. In fact, depending upon the molecular weight, viscosity and the extent of entanglement of polymer chains vary for a solution of fixed concentration. Under fixed concentration, by reducing the molecular weight of polymer, the morphology nanofibers will be changed from smooth fibers to beads. Whereas by increasing the molecular weight, continuous nanofibers will be formed (Fig. 2C).[27] However, too much increase in molecular weight results in the formation of micro-ribbons. Even for the case of lower solution concentration, if a polymer is of very high molecular weight, then it forms micro-ribbon like fibers. Hence, an optimum viscosity and specific molecular weights are essential to obtain uniform nanofibers.

Solution conductivity is an important factor exhibiting significant control on nanofiber diameter because, it can affect the Taylor cone formation. Taylor cone will be formed only when the solution is conductive. Indeed, in a nonconductive solution, there are no free moving charges to migrate to the surface and form a Taylor cone under the influence of applied electric field. Low conductive solutions also fail to form a Taylor cone due to lack of free moving charges. However, by increasing the conductivity of the solution to an optimal level, it is possible to make sufficient free charges available to interact with the external electric field to form Taylor cone. Once the stable Taylor cone is formed, the ejecting jets produce uniform and thin nanofibers. Conducting polymer solutions can establish electrostatic forces between charges and the applied electric field. For nonconducting solutions, a small amount of salt will be added to the solution, to induce free charges necessary for Taylor cone formation. In addition, if the solution's conductivity is below the optimum level, the tangential electric field acting along the surface of the solution decreases, which will disturb the formation of Taylor cone. Hence, ideal solution conductivity is essential to facilitate the formation of uniform nanofibers.[30]
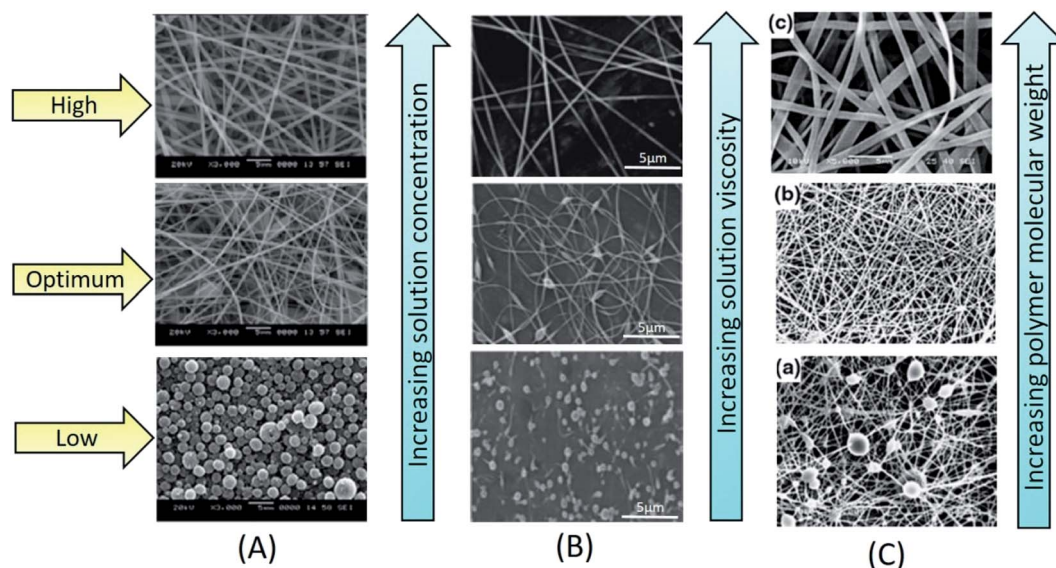

Fig. 2 Influence of solution factors on morphology of electrospun nanofibers; (A) influence of solution concentration on morphology of electrospun SAN nanofibers.[18] Reproduced from ref. 18 with permission from SAGE, copyright 2015. (B) Influence of solution viscosity on morphology of electrospun polyethylene oxide (PEO) nanofibers.[26] Reproduced from ref. 26 with permission from Wiley Periodicals, LLC., copyright 2015. (C) Influence of polymer molecular weight on morphology of electrospun PVA nanofibers.[27] Reproduced from ref. 27 with permission from Scientific. Net, copyright 2016.

Processing factors

Under processing factors, an applied voltage plays a key role in transforming a solution droplet at the tip of a spinneret into a Taylor cone, which is the preliminary step of jet formation. In fact, depending upon the nature of polymer solution (concentration, conductivity, viscosity, surface tension *etc.*) the range of an applied voltage will be varied from solution to solution. As the voltage increases, coulombic repulsion of charges within the jet will be increased. As a consequence, the jet will stretch and become thinner to form nanofibers. If the voltage is higher than the optimum range, leads to two types of structural transformations, either completely beads or beaded nanofibers (Fig. 3A) or from cylindrical nanofibers to flat thin nanofibers will be formed. These kinds of structural transformations can be attributed to the decrease of size of a Taylor cone with the increase of jet speed at higher voltages.[31]

Another important factor that decides the diameter and morphology of nanofibers is the flow rate of a polymer solution at which the solution enters the tip of a spinneret. If the flow rate is very low, sufficient amount of polymer solution cannot be supplied to the tip of a spinneret/needle to form a Taylor cone. If the flow rate is optimum, a stable Taylor cone will be formed, that finally results in uniform fiber formation, without any bead or spindle like structures. In case of lower flow rates, the jet undergoes proper drying and elongation, whereas in case of higher flow rates, beaded or bead-free thick nanofiber will be formed due to incomplete stretching and drying of the jet. Flow rate varies from solution to solution, depending upon the nature of polymer and the solvent used. Cai *et al.* studied the effect of flow rate on morphology and diameter of CPVC nanofibers. They found gradual increase in diameter of chlorinated poly(vinyl-chloride) CPVC nanofibers with the increase of flow rate from 0.2 mL h^{-1} to 1.0 mL h^{-1}, due to fiber adhesion caused by incomplete evaporation of solvent.[32] Similar effect of flow rate on nanofibers was also observed by Lin *et al.* for thermoplastic carboxymethyl cellulose[33] and by Li *et al.* for PVP nanofibers.[25] In addition, for some polymer solutions, the increase in flow rate could transform from more beaded nanofibers to nanofibers with less beads (Fig. 3B). The diameter of the electrospun nanofiber is more responsive to solution concentration and flow rate than an applied voltage and TCD.[17] It can increase the thickness or the number of beads, and in some cases, ribbon like microfibers can also be formed.[34] An unduly large increase in flow rate can also result in web like appearance of electrospun nanofibers.[35]

The TCD has a significant impact on morphology and diameter of nanofibers. Like other factors (concentration, applied voltage, viscosity, and flow rate), the TCD also changes depending upon the properties of a polymer solution. Depending upon the rate of solvent evaporation, deposition time, and whipping interval, the morphology and diameter of a nanofiber will vary with TCD.[36] Many studies revealed that the diameter of nanofiber decreases with increase of TCD. Matabola *et al.* studied the influence of TCD on PVDF nanofibers, by using 28 wt% PVDF solution at 12 kV and varying the distance from 15 cm to 16 cm. They found decreasing effect on diameter (from 397 nm to 314 nm) with increase of TCD, which was due to complete evaporation of solvent, and improved stretching and thinning of the polymer jet.[31] If the TCD is optimum, more
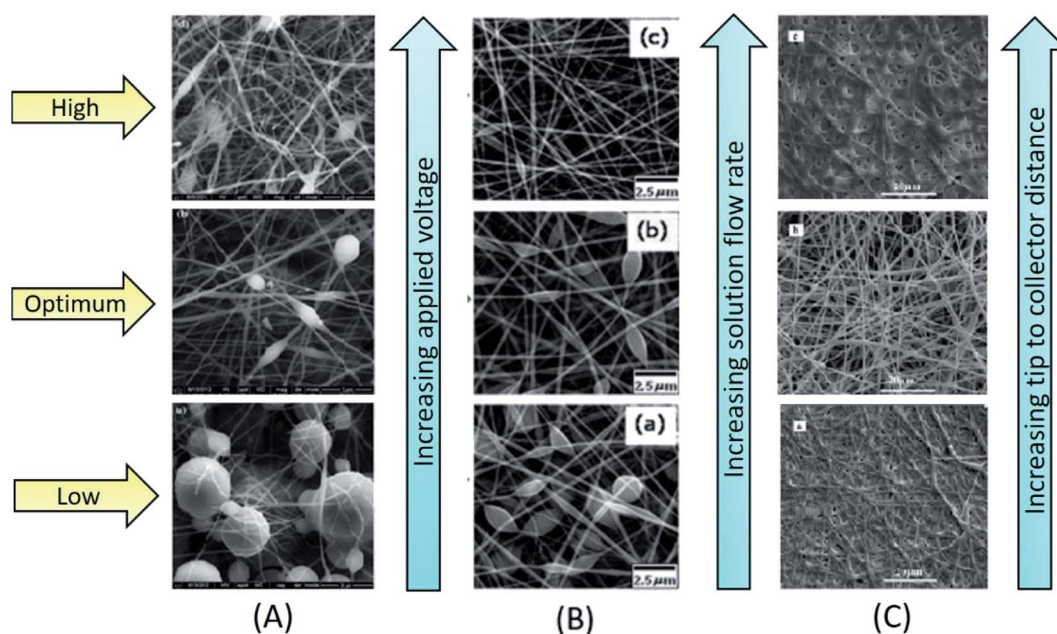

Fig. 3 Influence of processing factors on morphology of electrospun nanofibers; (A) influence of applied voltage on electrospun PVDF nanofibers.[31] Reproduced from ref. 31 with permission from Springer, copyright 2013. (B) Influence of solution flow rate on morphology of polyvinylpyrrolidone (PVP) nanofibers.[25] Reproduced from ref. 25 with permission from Wiley Periodicals, LLC., copyright 2014. (C) Influence of tip to collector distance on morphology of electrospun PVA/nickle oxide (NiO)-gadolinium-doped ceria (GDC) nanofibers.[41] Reproduced from ref. 41 with permission from Elsevier, copyright 2013.

uniform nanofibers will be formed, whereas defective or beaded nanofiber will be obtained when the distance is too long or too short.[16,37–39]

Also, it has been observed from several studies that the increase of TCD can also increase the diameter of nanofibers, due to decrease in strength of the electric field along the jet, which results in nanofibers of larger diameter.[40] Singh *et al.* prepared PVA/Zn-propoxide nanofibers at TCD range of 3.5–6.5 cm. The sizes of the obtained nanofibers were 170 nm to 550 nm at 3.5 cm and 325 nm to 855 nm at 6.5 cm. This was imputed to the decrease of electric field strength and electrostatic repulsive forces acting on the discharged polymer jet.[41] Some studies also reported that the TCD does not have any significant effect on diameter and morphology of nanofibers.[35] However, for a case of less volatile solvent, polymer jet loses solvent before reaching the collector. Hence, the increase in TCD has shown positive effect on solutions of low volatile solvents. The residual solvent carried by the nanofiber causes binding between individual layers of nanofiber and forms an interconnected network with improved mechanical strength. When TCD is optimum, nanofibers get sufficient time for solidification, which results in the deposition of separate and uniform continuous nanofibers on the collector. When TCD is higher, fiber diameter increases due to decrease in electrostatic force, leading to less stretching of nanofibers (Fig. 3C). Hence, in order to obtain smooth individual nanofibers with desired properties, it is necessary to optimize the distance between needle tip and collector.[42,43]

Ambient (environmental) parameters

The ambient parameters, such as relative humidity and temperature, also have a strong influence on morphology and diameter of electrospun nanofibers. In general, for a solution of optimum viscosity, low ambient humidity allows the formation of defect-free nanofiber and for a solution of higher viscosity; it allows discontinuous nanofiber formation with uneven surface. If the humidity is very high, electrospinning will not happen.

For a solution of hydrophilic polymer, the increase in relative humidity shows decreasing effect on the diameter of nanofibers. This happens in two different ways, either humidity will act as a plasticizing agent by reducing the crystal stability and enhancing the mobility of polymer chains and segments or it will hinder the fast evaporation of solvent by allowing the polymer jet for proper stretching and solidification during its flight. Pelipenko *et al.* studied the effect of increase in humidity on diameter of PEO, PVA, and blend solution of PVA/hydroxyapatite (Ha). They observed decreasing effect on diameter of nanofibers with the increase of humidity from 4% to 70%. They further extended humidity to higher level, and found that very higher humidity can transform morphology from nanofibers to beads (Fig. 4A–C).[44] In another report, for polyamide 46 (PA46) and polyamide 49 (PA69) solutions, an increase in humidity showed the decreasing effect on the diameter of a nanofiber. Moreover, the decrease in diameter was more pronounced for the case of PA46 compared to PA69. This was due to greater hydrophilicity and low crystal stability of PA46 compared to PA69; the absorbed water droplets caused the plasticizing effect, by reducing the fraction of stable crystals, which resulted in more stretching of PA46 polymer jet than that of PA69.[45] The humidity can affect surface as well as interior regions of nanofibers through various phenomena, depending upon the nature of the constituents in a solution. It can induce phase separation, precipitation, and surface charge imbalance due to exchange of charges from polymer solution to atmospheric humidity both in Taylor cone and in the jet regions.[46]

An optimal temperature is also essential for the production of electrospun nanofibers.[47] For a higher ambient temperature, nanofibers with larger diameter will be formed due to fast evaporation of solvent causing quick solidification of the jet. Oğulata *et al.* systematically investigated the effect of ambient humidity and temperature on the diameter and morphology of nanofibers of polyethylenimine/*N*-methyl pyrrolidone (PEI/NMP) solution by varying the solution concentration (18–20 wt%), TCD (12–18 cm) and applied voltage (15–25 kV). They
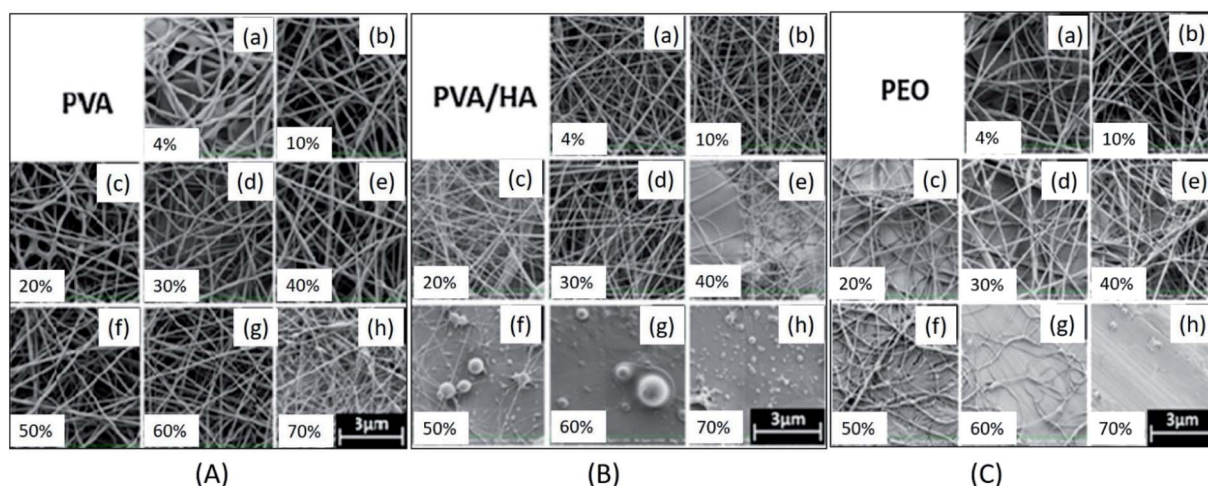

Fig. 4 Influence of increase of humidity level from 4% to 70% on morphology of electrospun nanofibers; (A) PVA nanofibers, (B) PVA/HA blend nanofibers, (C) PEO nanofibers. Reproduced from ref. 43 with permission from SAGE, copyright 2015.

found maximum increase in fiber diameter for 20% PEI solution at the range of relative humidity (RH) 30–70% and temperature at 15–35 °C and lowest diameter at 15–35 °C for all the humidity levels used.[38] Hence, both the optimum relative humidity and temperature are necessary to obtain defect free nanofibers.

Recent advances in electrospinning to fabricate electrospun nanofiber membranes (ENMs)

Electrospinning has been widely considered as the most efficient technique for producing micro and nanofibers from variety of materials to fabricate water filtration membranes. Careful optimization and control of limiting factors of conventional needle electrospinning can enable the fabrication of highly interconnected pore structured defect free nanofiber membranes.[48–51] By varying the solution concentration, the diameter of the nanofiber can be increased or decreased, inorder to optimize the membrane thickness and pore size distribution to achieve better filtration efficiency. For example, Wang et al. fabricated PAN ENM as a barrier layer on PET non-woven support layer to obtain a microfiltration (MF) membrane. They

studied the effect of solution concentration on fiber diameter and correlated with the membrane thickness and pore size distribution. They observed that at lower concentrations the solution was not viscous enough to form stable fiber jets. They also found that at optimum solution concentration, the nanofibers of smaller diameter were formed, which led to small interconnected pores distributed uniformly in the membrane.[52] Other than solution factors, the processing factors also have shown significant effect on properties of ENMs, the variation in applied voltage can influence the morphology of nanofiber, whereas the variation in TCD can influence the pore size of ENM by affecting the diameter of nanofibers. For example, T Mazoochi et al. investigated the effect of processing factors including applied voltage and TCD on the structural properties of PSf ENMs. They observed that TCD has direct effect on jet flight time and solvent evaporation time, and also increases electric field strength, leading to the formation of beaded fibers. Whereas the longer TCD resulted in uniform continuous nanofibers. They also found that the effect of TCD was more pronounced at higher applied voltages. Higher applied voltage increased the surface charge of the jet and helped to reduce the frequency of formation of beads in the nanofibers.[53] The ambient factors such as temperature and relative humidity (RH) also influence the properties of ENMs, the temperature has
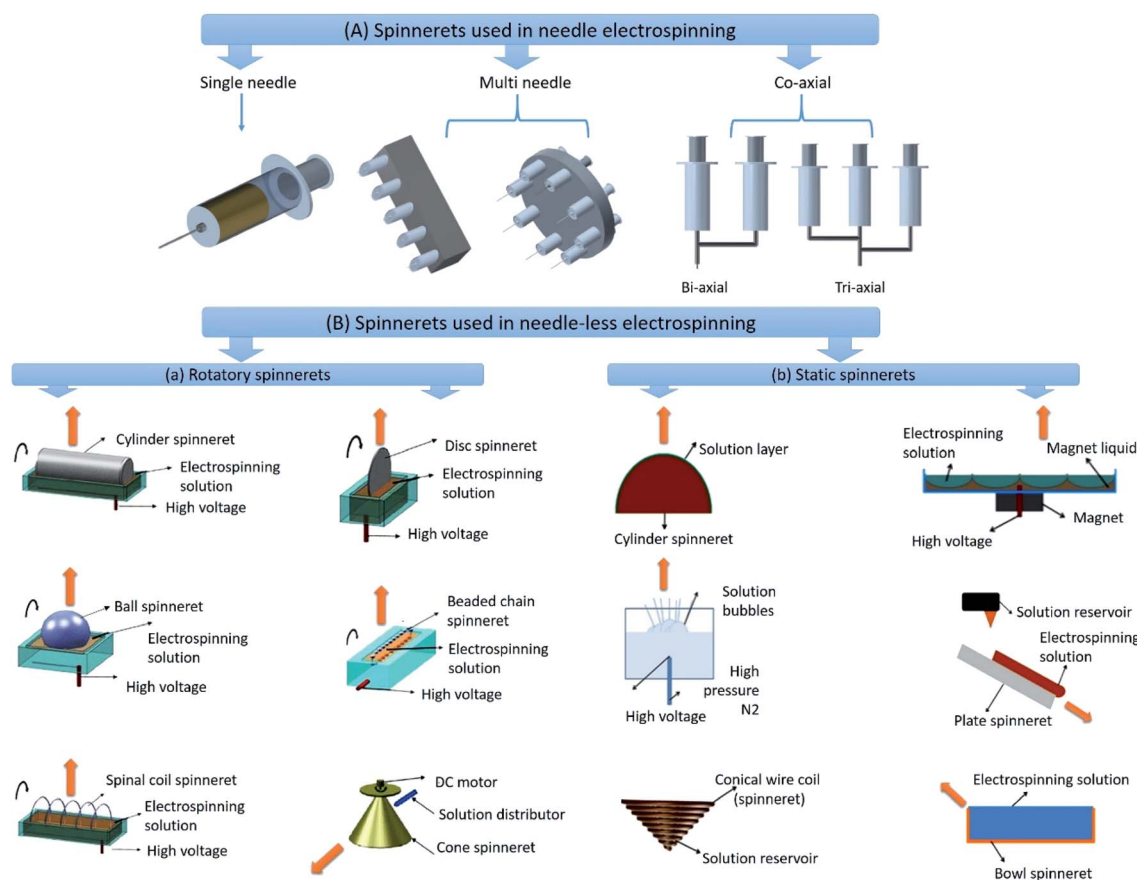

Fig. 5 Different types of spinnerets used in electrospinning; (A) spinnerets used in needle electrospinning. (B) Spinnerets used in needle-less electrospinning; (a) rotary spinnerets and (b) stationary spinnerets used in needle-less electrospinning. Reproduced from ref. 47 with permission from American Chemical Society, copyright 2014.

direct influence on solution viscosity and solvent evaporation and RH can greatly influence the solvent evaporation, therefore these two factors have significant control on the nanofiber formation and nanofiber diameter.[54] Tang *et al.* studied the influence of RH on morphology of PES ENMs. They observed that the diameter of the nanofibers increased from 266 nm to 492 nm with the increase of RH from 45% to 70%. In addition to the optimization of limiting factors, the thickness of the membrane can also be optimized by varying the duration of electrospinning under optimum conditions. By controlling the thickness of an ENM; the pore size, liquid entry pressure (LEP) and tortuosity of an ENM can be optimized to achieve higher filtration efficiency.[55] However, the conventional single-needle electrospinning exhibits several drawbacks such as low productivity, clogging at the spinneret tip, irregular distribution of components within the fiber, inefficiency to control the architecture of the fabricated material due to random orientation of nanofibers on the collector. Therefore the conventional single needle electrospinning is convenient only for the laboratory scale fabrication of ENMs.

The recent advancements in electrospinning have not only broadly expanded the availability of nanofibers with variety of morphology but also enabled controlling the orientation of nanofibers in the required pattern with enhanced productivity. The advancements in spinneret components of the needle electrospinning setup such as multi needle and co-axial spinnerets (Fig. 5A) have enabled the faster production and large area deposition of nanofibers. The multi needle spinnerets offer an advantage of fabricating ENMs consisting mixed nanofibers originated from different polymer solutions, the mixing of nanofibers takes place due to the interference occurred during electrospinning process.[56] The co-axial spinnerets have been used to fabricate hollow, core–sheath and composite nanofibers based ENMs *via* simultaneous electrospinning of two or more dissimilar polymer solutions by feeding through the spinneret system with coaxial capillaries. The ENMs of hollow nanofibers can be obtained *via* removal of the core component of the fibers.[57]

Over the last decade, for large scale and cost effective production of ENMs, needle-less electrospinning has been emerged as the most suitable approach. In this approach,
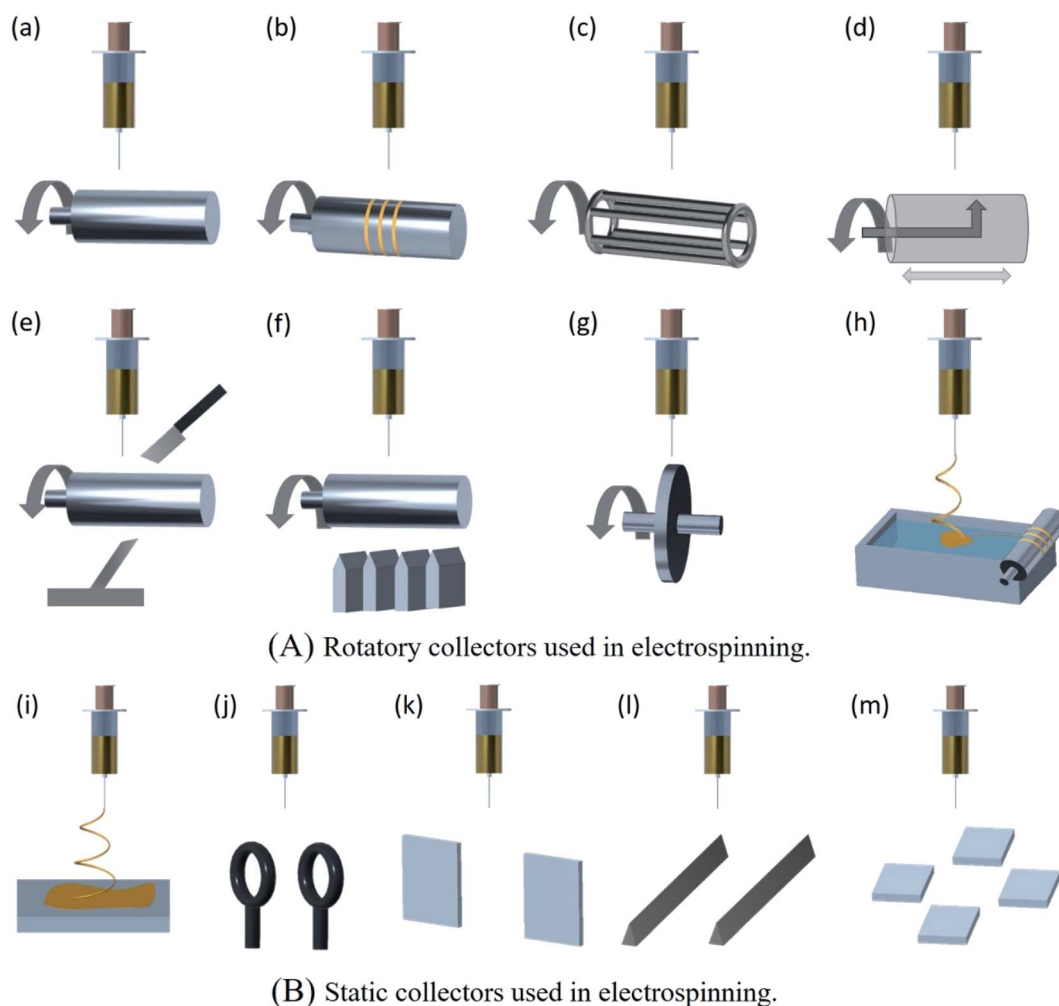

Fig. 6 Different types of collectors used in electrospinning; (A) rotatory collectors (a–h), (B) static collectors (i–m); (a) rotating drum, (b) rotating drum with wrapped wire, (c) rotating wire drum, (d) rotating drum with sharp pin inside, (e) rotating drum with knife edge electrodes, (f) rotating drum with multiple knife edge electrodes, (g) rotating disk, (h) fiber collection using water bath, (i) plate collector, (j) parallel ring collector, (k) blade electrodes in line, (l) parallel electrodes, (m) array of counter electrodes.

different shapes of spinnerets other than needle have been used and are classified as rotatory spinnerets and static spinnerets. The different types of rotatory and static spinnerets are presented in the Fig. 5B.[58] The rotatory spinnerets include rotary cylinder, ball spinneret, spinal coil spinneret, rotary disc, moving bead chain, and rotary cone.[59] Except rotary cone, the other rotatory spinnerets are partially immersed in the polymer solution, and nanofibers are electrospun upward inorder to prevent dripping of polymer solution onto the nanofibers deposited on the collector, this results in the formation of high quality nanofiber membranes. The rotation of spinnerets continuously supplies polymer solution to the electrospinning sites to maintain the continuous production of nanofibers. The main advantage of needle-less electrospinning is that the multiple nanofiber jets are initiated naturally in the optimal positions at the surface of the rotating spinnerets.[59] These spinnerets eliminate clogging problems and also enable faster production as well as larger area deposition of nanofibers.[60] Industrial needle-less electrospinning plants of Inovenso Ltd., IME Technologies, and Elmarco have the capacity to produce in several kilograms per hour.[61] It mainly depends upon the number of spinnerets involved in electrospinning and also number of jet initiation points originated on the free surface of the spinneret. However, it is difficult to produce well aligned, uniform and different shapes of nanofibers in needle-less electrospinning.[62]

In electrospinning technology, controlling an alignment of nanofibers in a required direction is extremely important. To improve the control on nanofiber alignment, different types of collectors have been developed. As shown in Fig. 6, the electrospinning collectors are broadly categorized as rotatory collectors and static collectors. Rotating drum collector can be used to align large amount of nanofibers. However, it doesn't provide highly aligned nanofibers and it requires an optimization of drum rotation speed, since the high speed drum rotation can cause breakage of nanofibers.[63] Rotating wire drum collector can lead to highly aligned nanofibers, and thick layer formation of deposited fibers is the drawback, after certain thickness of fiber deposition, the alignment and orientation of fibers may not be appropriate.[64] A rotating drum with sharp pin inside can be used to obtain large area aligned nanofiber mats, this type of collector is generally used to fabricate thin mats of aligned nanofibers.[65] A rotating drum collector with knife edge electrodes is used to deposit highly aligned nanofibers. As the entire deposition is highly aligned, it is easy to obtain thick mats of deposited nanofibers.[66] A rotating drum wrapped with wire wound collector can be used to obtain highly aligned nanofiber membranes, in this collector the area of deposition of nanofibers can be controlled by varying the thickness of the wire.[67] A rotating disc collector is also used to obtain highly aligned nanofibers. However, the disc rotation speed needs to be optimized to avoid breakage of nanofibers and the drawback is only smaller area of aligned nanofiber mats can be obtained.[68] In case of water bath collector, the polymer solution is electrospun into water bath for solidification of nanofibers, and then the solidified nanofibers are twisted and aligned into yarns using a rotating drum collector.[69] A static collector like plate

collector results in a randomly aligned nanofiber mats, and parallel ring collector enables to fabricate nanofiber yarns with twisted pattern. However, inorder to obtain twisted yarns one of the rings has to be rotated and only the limited length of twisted yarn can be obtained.[70] Parallel electrode collectors produce highly aligned nanofibers and the obtained nanofibers can be easily transferred to different substrates. However, it is difficult to obtain thicker deposition and lengthy nanofibers.[71] In certain cases, by adding a small quantity of magnetic nanoparticles into polymer solution and then by electrospinning under an external magnetic field, the nanofibers can be stretched along the gap between the collectors to obtain unidirectional array of nanofibers.[72]

Polymeric ENMs to expel pollutants from aqueous system

The progress in the area of ENMs since last decade has significantly transformed the sense of membrane fabrication. Due to the advantages such as (i) ability to exhibit high rejection efficiency and permeate flux while operating under low pressure owing to the high interconnected porosity and (ii) ease of surface modification through various physical and chemical methods such as, heat treatment, plasma treatment, functionalization, crosslinking, doping and oxidation, the ENMs have exhibited significant contributions in different areas of water treatment. The Table 1 contains some examples of polymeric ENMs that have been used in various water treatment applications. The potentialities of various polymeric ENMs to expel a large variety of pollutants from aqueous system are more specifically detailed in the following paragraphs.

ENMs in microfiltration process

A membrane with uniform pore size, better mechanical strength and desired thickness can be fabricated by electrospinning. Thus, electrospun nanofibrous membranes appear as a suitable alternative to conventional phase inversion membranes. By tuning the parameters of electrospinning, the pore size of a microfiltration membrane can be tuned depending upon the application's requirement. The ideal pore size of an electrospun microfiltration membrane is smaller than 0.2 mm and potentially used to remove micro and sub micro pollutants such as mud and suspended micro particles, and importantly for removal of various types of microorganisms from water (Fig. 7). Liu *et al.* prepared a microfiltration ENM using PVA solution and glutaraldehyde as a crosslinking agent. The resultant ENMs were able to provide pure water flux 3–7 times higher than the Millipore GSWP membrane (pore size – 0.22 mm) and >98% rejection of polycarboxylate microsphere particles (with size of 0.2 mm).[106] In another report, an electrospun M-aramid membrane showed significantly higher particle rejection (nearly 100%) of PS latex beads (0.20 μm). Which is greater than the efficiency of commercial GSWP filter to reject PS latex beads (*i.e.* 95.91%).[107] Bae *et al.* fabricated PES nanofibrous membrane by electrospinning using NMP as a solvent. They obtained membranes of pore size around

Table 1 Examples of some of the previously reported polymeric ENMs that have been used in various water treatment applications

Sl. no	Electrospinning solution used (polymer and solvent)	Experimental variables (concentration, TCD, needle diameter, applied voltage, flow rate)	Properties of ENMs (average fiber diameter (nm), surface area (m² g⁻¹), weight of fiber (g m⁻²))	Application of ENMs
1.	Cellulose triacetate (CTA), dichloromethane (DCM)/ethanol/pyridine & DCM/EtOH	8/1/1(v/v/v)% & 8/2(v/v)%, 10 cm, 0.52 mm, 25–27 kV, 10 mm³	340 ± 110 nm,	Desalination[73]
2.	Polystyrene (PS), DMF + 0.1 mL of nitric acid	20 wt%, 0.25 mm, 5 kV, 180 mL h⁻¹,	317 nm, 81.51 m² g⁻¹	Oil/water separation[74]
3.	Polylactic acid (PLA) (4060D320kD), acetone	11–13 wt%, 10 cm, 20 kV, 0.5 mL h⁻¹	500–1200 nm	Microfiltration[75]
4.	PVA, DI water	6–12 wt%, 10 cm, 1 mm, 24–32 kV, 10 mL min⁻¹	100 ± 19 nm	Microfiltration[76]
		10 wt%, 15 cm, 30 kV, 40 mL h⁻¹, with TritonX-100 (0.6 v/wt%)	120 ± 30 nm	Desalination[77]
		8 wt%, 12 cm, 0.8 mm, 15 kV, 1 mL h⁻¹	50–90 nm	Dye degradation[78]
		10 wt%, 15 cm, 0.5 mm, 17.5 kV, 1 mL h⁻¹,	180–280 nm, 130.513 m² g⁻¹, 88.946 m² g⁻¹	Heavy metal removal[79]
5.	PVP, absolute ethanol	10 wt%, 14 kV, 1 mL h⁻¹, with aluminium acetate	200–600 nm	Heavy metal removal[80]
		10 cm, 8–12 kV, 0.3 mL h⁻¹, with TiO₂ and Au NPs.	30–210 nm	Photoactive nanofiber water treatment[81]
6.	Polysulfone (PSF), DMF	15–20 wt% + NaOH (0–2.5 wt%), 15 cm, 20 kV, 20 wt%, 15 cm, 20 kV	130–630 nm	Oil–water separation[82]
7.	PAN, poly(ethylene glycol) diacrylate (PEGDA), 1-hydroxycyclohexyl phenyl ketone (HCPK), sodium dodecyl sulfate (SDS), DMF, DCM, hexane	PAN/PEG (8/0 to 12/2 wt/wt%), 15 cm, 20 kV, 1 mL h⁻¹	63 nm, 128 nm, 157 nm, 228 nm	Oil–water separation
	PAN, DMF, acetic acid	8 wt/wt%, 15 cm, 0.7 mm, 30 kV, 40 mL m⁻¹, with tetra ethyl orthosilicate (TEOS)	120.6 ± 30.2 nm, 225 ± 38.5 nm	Pressure retarded osmosis
	Poly(m-phenylene isophthalamide) PMIA, lithium chloride (LiCl)/DMAc	2.80 wt%, 15 cm, 30 kV, 0.15 mL h⁻¹	134 nm, 57.87 m² g⁻¹	Oil–water separation
	PVDF, DMF	8 wt%, 12–15 cm, 27–30 kV, 30 mL min⁻¹	300–400 nm,	Forward osmosis[83]
8.	Polyethylene terephthalate (PET) & PVA, trifluoroacetic acid (TFA) & DI water	PET 13.5 wt% in TFA & PVA 7 wt% in DI water, 0.7 mm, 20 kV, 13.5 mL min⁻¹	—	Desalination[84]
	PAN, DMF	8 wt%, 15 cm, 0.7 mm, 22 kV, 20 mL min⁻¹, with MWCNTs	300 nm, 250 nm	Ultrafiltration[85]
		6–12 wt%, 18 cm, 25 kV, 1 mL h⁻¹, with Jute cellulose nanofibers	173 nm, 18.83 m² g⁻¹, 17.02 m² g⁻¹	Water purification[36]
		10 wt%, 28 kV, 1 mL h⁻¹	270 ± 55–281 ± 65 nm, 460 ± 240–450 ± 210 nm	Water purification[86,87]
		4–18 wt%, 7–19 cm, 0.6 mm, 27 kV, 0.5–2.5 mL h⁻¹	100–500 nm, 40 m² g⁻¹	Microfiltration[88]
		12 and 8 wt%, 10–18 cm, 15 kV, 10–20 mL h⁻¹	150–300 nm	Oil–water separation[89]
10.	PAN/poly(amidoamine) (PAMAM), DMF	PAN = 10 wt%, PAMAM = 5–30 wt%, 16 cm, 16–23 kV, 1.2 mL h⁻¹	240–355 nm, 30.4 m² g⁻¹, 26.2–12 m² g⁻¹	Dyes removal[90]
11.	PAN/PSf, DMAc	PAN = 10 wt%, PSf10 wt%, PAN/PSf 15 wt% with different weight ratio, 15 cm, 25 kV, 1.5 mL h⁻¹	879 ± 37 nm, 364 ± 52 nm, 7–27.5 m² g⁻¹	Adsorptive removal of lanthanum(III) ions[91]

Table 1 (Contd.)

Sl. no	Electrospinning solution used (polymer and solvent)	Experimental variables (concentration, TCD, needle diameter, applied voltage, flow rate)	Properties of ENMs (average fiber diameter (nm), surface area ($m^2\ g^{-1}$), weight of fiber ($g\ m^{-2}$))	Application of ENMs
12.	Cellulose acetate (CA), DMF/acetone	CA = 6–14 wt%, 12 cm, 0.4 mL h^{-1}	170 ± 40 nm	Optical, bactericidal and water repellency[92]
13	CA, acetic acid/DI water	8 g in 42 mL co-solvent mixture, 15 cm, 0.8 mm, 23 kV, 1 mL h^{-1}	222 ± 130 nm, 213 ± 116 nm	Virus removal[93]
14.	Polyether sulfone (PES), NMP	9–22 wt%, 10 cm, 0.8 mm, 18–30 kV, 20 mL min^{-1}	1090 nm, 700 nm, 610 nm	Microfiltration[94]
15.	PU, PES, DMF, DMAc, dimethyl sulfoxide (DMSO), NMP	PU-(14–18) wt% & PES (15–20) wt%, 10–12 cm, 25–35 kV, with Ag nanoparticles	205 ± 67 nm, 174 ± 51 nm, 6.5–7.2 g m^{-2}	Biocidal membrane for ultrafiltration[95]
16.	PVDF, DMF	18 wt%, 18 cm, 18 kV, 2 mL h^{-1}	417 ± 120, 625 ± 13 nm	Water treatment[96]
17.	PVDF, DMAc/acetone	15 cm, 1 mm, 13 kV, 0.055 mL min^{-1}	0.57–0.61 μm	Ultrafiltration[97]
18.	PVDF, DMF/tetrahydrofuran (THF)	13 wt%, 15 cm, 20 kV, 1.5 mL h^{-1}	860 ± 350 nm, 930 ± 280 nm	TFC membrane[98]
19.	Poly(acrylonitrile-co-glycidyl methacrylate) PANGMA, DMF	20 wt%, 25 cm, 15–20 kV, 1.1 mL h^{-1}	100–126 nm	Protein and enzyme separation from water[99]
20.	Nylon-66, formic acid/DCM	10 wt%, 8 cm, 28 kV, 0.8 mL h^{-1}	270 ± 120 nm	Engineered osmosis[100]
21.	PU, THF/DMF	10 wt%, 15 cm, 20 kV, 0.3 mL h^{-1}, with Ag-TiO$_2$ nanostructures	550 nm, 80 g m^{-2}	Photo catalytic treatment of dairy effluent[101]
22.	PEI, DMF/NMP	20 wt%, 10 cm, 25 kV, 1 mL h^{-1} SiO$_2$, BaTiO$_3$, Si$_3$N$_4$	636 nm to 3.47 μm, 0.71–5.64 g m^{-2}	Microfiltration[102]
23.	Chitosan (CS), acetic acid	5 wt%, 6.8 cm, 23 kV, 0.1 mm min^{-1}	75 nm, 0.18–2 g m^{-2}	Heavy metal removal[103]
24.	Chitosan (CS), acetic acid	0.4 wt%, 7 cm, 0.2 mm, 8 kV, 0.8 mL h^{-1}	42 nm, 110 $m^2\ g^{-1}$	Heavy metal removal[104]
25.	PVA, DI water	18 wt%, 6 cm, 10 kV, 2.5 mL h^{-1}	400 nm, 7.55–10.79 $m^2\ g^{-1}$	Heavy metal and dyes removal[105]

4175 nm and particle rejection and flux performance of eight times higher than the commercial electrospun nanofibrous membranes.

Moreover, due to low volatility of NMP, residual solvent present in the fibers caused the fusion of inter nanofibrous junctions, thereby increasing the mechanical properties (tensile strength around 11 MPa) and surface roughness.[108] The microfiltration membrane with mean pore size of 0.22–0.01 μm was prepared by Sadasivam et al. by fabricating electrospun PAN nanofibers on to a PET nonwoven substrate, which showed significantly better performance than the commercial microfiltration membrane by maintaining high flux with >99% of bacterial (Escherichia coli) rejection.[109] In another study, PAN/PET microfiltration membranes functionalized by impregnation of cellulose nanowhiskers and PAN membrane surface functionalized by dual-vinyl and tri-vinyl monomers have shown better water treatment ability and complete rejection of Escherichia coli by size exclusion.[110] However, the microbial layer formation on the surface of the membranes (bio-fouling) often inhibits the flux performance of the microfiltration membranes. Therefore, the microfiltration membranes with

negative surface charge have been used to prevent biofouling. The negative charge on the membrane's surface induces electrostatic repulsion between the micro-organism and the membrane's surface, and therefore prevents the adhesion of microbes to the surface of the membrane. For example, Liu Ying et al. fabricated PVA-co-polyethylene (PE) based anti-fouling microfiltration ENMs for water treatment application. The membrane was first activated by tricyanogen chloride (TC), followed by PEI grafting, which was further coated by citrate capped silver nanoparticles (Ag NPs).[111] The resultant membranes showed complete rejection of E. coli and S. aureus cells, with stable water flux. Moreover, the membranes showed excellent inactivation performance for bacteria with antimicrobial rate of >99% (Fig. 8).

Most of the microfiltration membranes are prepared by using commodity polymers. However, these polymers are often hazardous to environment due to their non-degradability and toxicity. To avoid such negative impacts of commodity plastics, innovative eco-friendly polymers, derived from renewable resources have been demonstrated. For example, L. Li et al. fabricated microfiltration membrane using electrospun PLA nanofiber mats modified by annealing treatment. After
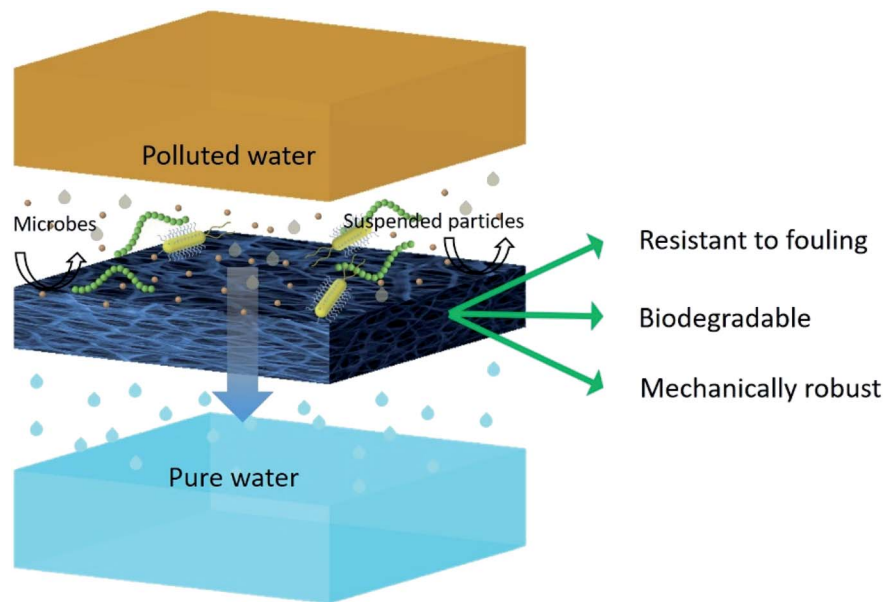
Fig. 7 Schematic representation of removal of micro-pollutants from water by filtration through an ideal ENM.

annealing treatment, they observed an improvement in both mechanical properties and solid micro particles rejection performance of the PLA membranes.[112] Lee A *et al.* fabricated the electrospun microfiltration membranes of cellulose acetate (CA) nanofibers coated with chitin nanocrystals. The infusion of chitin nanocrystals to cellulose acetate nanofibers not only decreased the bio-fouling tendency but also induced the superhydrophilicity to membranes, making them suitable for high flux water purification processes.[113] However, innovative microfiltration ENMs are still needed to significantly replace non-degradable commodity polymer based microfiltration membranes by eco-friendly, anti-fouling and high permeability microfiltration ENMs.

ENMs in membrane distillation (MD)

More than 40% of the world's population is suffering from lack of access to fresh water. The smallest portion (0.01%) of the earth's water is fresh and it is unevenly distributed, the remaining portion of the earth's water is saline (about (97%). Hence, there is a tremendous need of efficient desalination techniques in order to overcome the scarcity of fresh water and to sustain the fresh water sources such as ground water, river, ponds, and lakes to maintain equilibrium between humanity and environment. Desalination is a process of removal of salts and various minerals from water. There are various methods of desalination such as, distillation techniques (vacuum distillation, multi-stage flash distillation,[114] multiple effect distillation,[115] and vapour compression) and membrane filtration techniques such as membrane distillation (MD),[116] reverse osmosis (RO),[117] and forward osmosis (FO).[118]

Thermally driven membrane based water purification technologies are extremely important to overcome global fresh water crisis. However, most of these technologies are energy exhaustive due to their inefficiency to utilize input thermal energy, due

to loss of heat energy through conduction, convection, temperature polarization (TP) and high energy requirement for water circulation. Also, their applications are attractive within the academic community but not for an industrial scale and long term usage. Thus, developing a new membrane technology which demands less pressure, temperature, and low cost of maintenance have become crucial to full fill large scale fresh water demand.[119] On the other hand, with increasing demand of fresh water due to increasing population and industrialization, the membrane technology started progressing from high pressure driven Reverse Osmosis (RO) to membrane distillation (MD), *i.e.* separation process that involves thermally driven transport of liquid vapour through a porous hydrophobic membrane that utilizes the vapour pressure difference between the two sides of the membrane as a driving force.[120] MD is the only process, where waste heat energy of a feed solution can be used to create vapour pressure gradient as driving force for vapour transportation across the membrane. As a result, different MD configurations have been emerged, namely direct contact membrane distillation (DCMD),[121] vacuum membrane distillation (VMD),[122] sweeping gas membrane distillation (SGMD)[123] and air gap membrane distillation (AGMD).[124] This further enhanced the desalination, effluent recycling, radioactive waste treatment, concentrating non-volatile compounds, and food-medical applications of thermally driven membrane separation technology. Though, the MD performance seems very favourable at the research level, many attempts on industrial scale applications have failed due to challenges in engineering aspects, durability issues, membrane wetting and fouling, noneconomic costs of membrane modules.[125] Moreover, MD is suitable for application only where feed solution is hot, otherwise heating a bulk feed will consume high amount of energy. Developing some cost-effective and energy-efficient membrane modules to introduce innovative MD units need to be largely explored.[126]
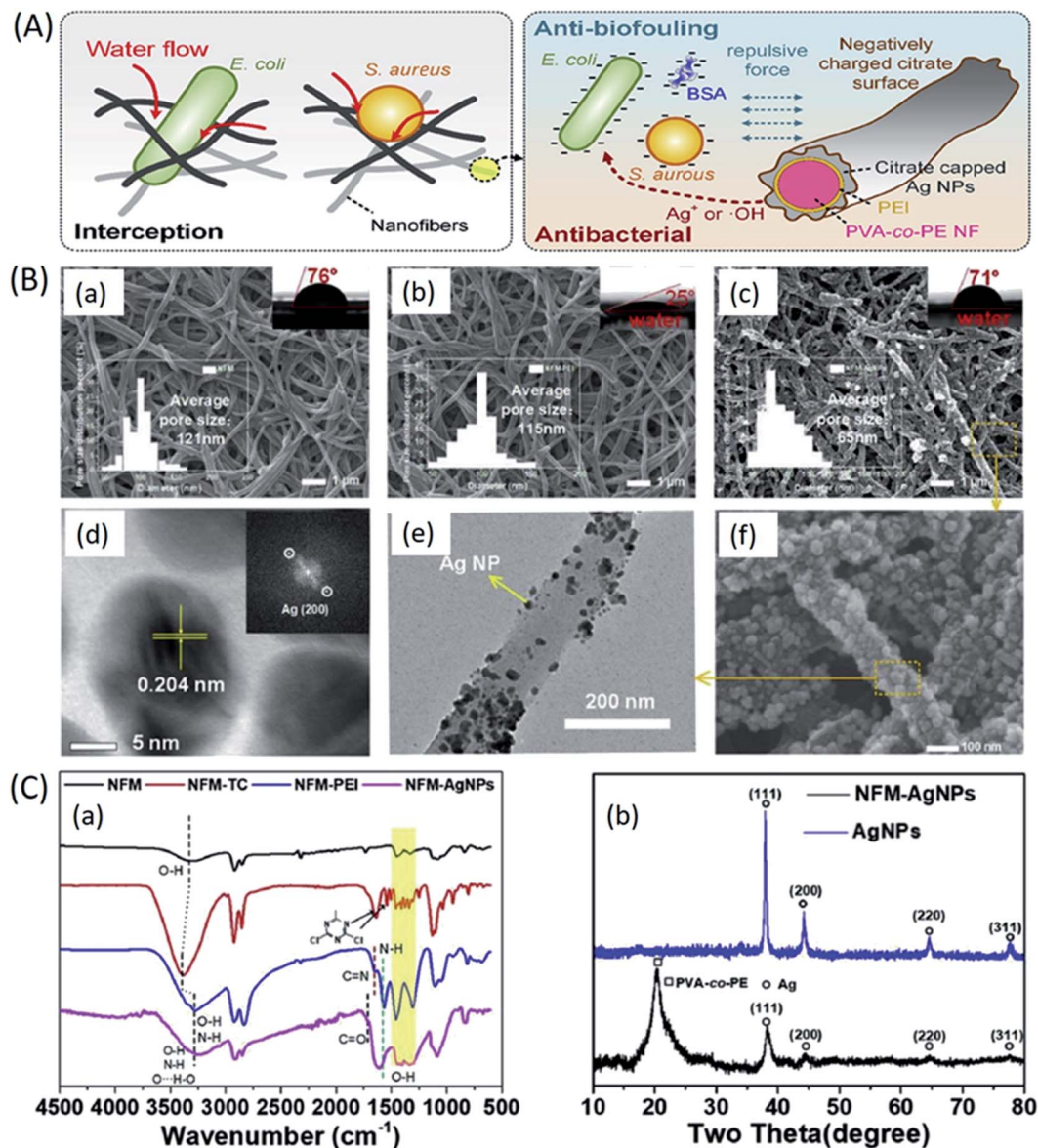
Fig. 8 PVA-*co*-PE based anti-fouling microfiltration ENMs for water treatment application; (A) mechanism of interception, anti-biofouling, and antibacterial behaviour of PVA-*co*-PE-PEI-Ag NPs ENMs, (B) SEM, contact angle (CA) and pore size distribution of; (a) PVA-*co*-PE, (b) PVA-*co*-PE-PEI, and (c) and (f) PVA-*co*-PE-PEI-Ag NPs ENMs, (d) HRTEM and its FFT image of immobilized Ag NPs, (e) TEM image of PVA-*co*-PE-PEI-Ag NPs ENMs, (C) chemical characterization; (a) FT-IR spectra of PVA-*co*-PE, PVA-*co*-PE-TC, PVA-*co*-PE-PEI, and PVA-*co*-PE-PEI-Ag NPs ENMs, and (b) XRD patterns of PVA-*co*-PE-PEI-Ag NPs ENM and Ag NPs.[111] Reproduced from ref. 111 with permission from Elsevier, copyright 2020.

In the recent developments, with the advent of innovative production techniques and in order to fabricate membranes that can full-fill necessary characteristics particularly for MD application, modified membranes have been explored essentially with the aim of enhancing permeability wetting resistance and thermal resistance.[127] Tremendous progress in nanotechnology has created a broad platform in the development of MD membranes. Generating nanofibers from polymer solution using electrospinning technique has gained remarkable interest as it can be used to fabricate membranes with high interconnected porosity, mechanical stability, tuneable hydrophobicity and thickness.[128] ENMs have been extensively studied for MD performance. For the first time, Feng *et al.*

demonstrated electrospun PVDF membranes for AGMD process. Later, Essalhi *et al.* systematically studied the influence of polymer concentration and thickness of the membrane on desalination *via* DCMD process. They fabricated PVDF nanofibrous membranes from solutions of varying concentrations. The resultant membranes showed rejection factor of about >99.99 for feed stream of 3 wt% NaCl.[129] In order to improve MD performance efficiency of ENMs, several modifications have been reported, such as hot press treatment,[130] loading non-functionalized/functionalized nanomaterials,[131,132] blending approach,[133] surface modification[134,135] and so on. Heat pressing is a post-treatment method used to enhance the mechanical and morphological properties of ENMs; by treating them with

certain pressure and temperature for fixed duration, without sacrificing their hydrophobicity and porosity. Liao *et al.* systematically studied the effect of heat-press post treatment and electrospinning process variables (spinneret moving speed, humidity, and polymer dope compositions containing inorganic additives) on the pore size distribution and DCMD performance of PVDF electrospun nanofibrous membranes.[136] The same research group recently proposed for the first time, a facile approach to fabricate a dual layer silica/PVDF microporous composite membrane by electrospinning, and the membrane performances were superior to previously reported conventional PVDF nanofibrous membranes.[137] Incorporation of functionalized nanomaterials help for enhancing the MD performance of ENMs, by tuning the roughness and surface chemistry (anti-wetting properties) of ENMs. For example, A.K. An *et al.* incorporated PFTS modified TiO_2 nanoparticles into PH ENMs to improve both hydrophobicity and DCMD performance (Fig. 9A). The resultant membranes showed improved

mechanical stability and better performance of treating high salinity water (7 wt% NaCl, which is equal to RO concentrate).[138] Li *et al.* incorporated octadecyltrichlorosilane (OTS) modified SiO_2 nanoparticles to improve the superhydrophobicity of PVDF ENMs for DCMD performance. Their membranes showed 5–6 times higher vapour flux than the commercial PVDF membranes (Fig. 9B). Recently, for VMD application Z.Q. Dong *et al.* developed a superhydrophobic (contact angle (CA) of 158°) membrane by grafting fluoroalkylsilane (FAS) on glutaraldehyde cross-linked electrospun PVA nanofiber, their membranes were chemically stable and showed (70%) better performance than a commercial polytetrafluoroethylene (PTFE) membrane for high salinity water desalination.[139] The same research group developed an even more superhydrophobic (CA of ≈161°) PVDF-silicon dioxide (SiO_2) ENMs by doping FAS-SiO_2 nanoparticles (from 0 to 8 wt%) into PVDF solution. They found that for VMD application, the resultant PVDF-SiO_2 ENMs with higher content of FAS-SiO_2 nanoparticles were highly resistant to
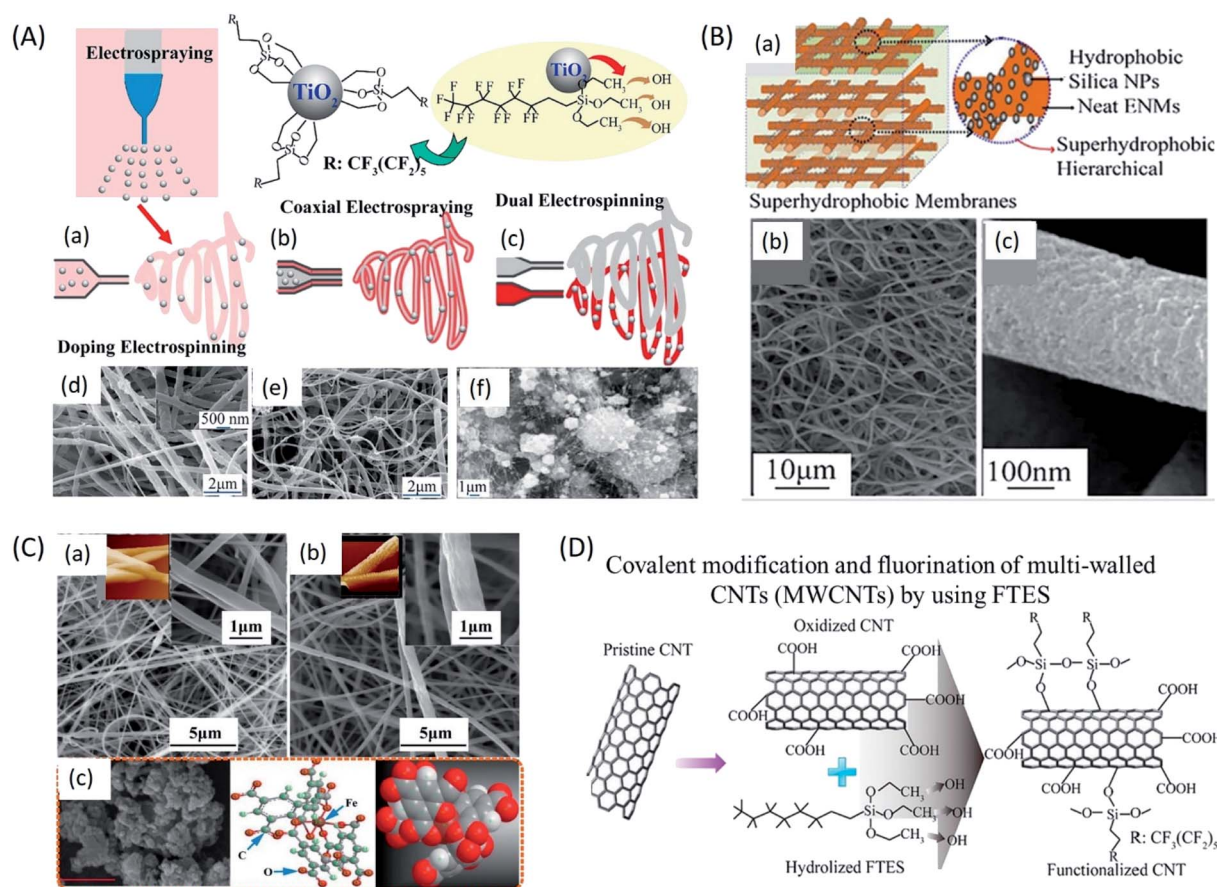

Fig. 9 Different functionalized nanomaterials for the preparation of doped electrospun nanofiber membranes for MD application; (A) schematic representation of preparation of 1*H*,1*H*,2*H*,2*H*-perfluorooctyltriethoxysilane (PFTS) functionalized TiO_2 nanoparticles through different methods like (a) direct doping, (b) co-axial electrospraying, (c) dual electrospinning, and electrospinning combined with electrospraying; and SEM images for TiO_2-polyvinylidene fluoride-*co*-hexafluoropropylene (PH) ENMs fabricated by (d) doping electrospinning, (e) coaxial electrospinning, and (f) dual electrospinning. (B) Superhydrophobic PVDF ENMs for DCMD application; (a) diagrammatic representation of octadecyltrichlorosilane (OTS) modified SiO_2 nanoparticles incorporated superhydrophobic PVDF ENMs for DCMD application; (b) and (c) SEM images for SiO_2-PVDF ENMs. (C) Metal organic framework (MOF-F300) incorporated PVDF ENMs (d) for DCMD performance; (a), (b) and (c) SEM images of MOF-F300-PVDF ENMs. (D) Schematic of covalent modification and fluorination by using FTES of multi-walled CNTs (MWCNTs) to construct 3D PH ENMs for DCMD application.[72] Reproduced from ref. 72 with permission from Elsevier, copyright 2019.

wetting compared to membranes with lower FAS-SiO$_2$ content. All PVDF ENMs with or without FAS-SiO$_2$ displayed a doubled salt rejection performance compared to a commercial PTFE membrane for a feed solution of 3.5 wt% NaCl. In another recent research, metal organic framework (MOF-F300) was incorporated to PVDF ENMs (Fig. 9C) for DCMD performance for treating 3.5 wt%. NaCl feed solution. MOFs doping imparted superhydrophobicity (CA of 138°) with the increase of surface roughness from 285.28 to 661.80 nm. As a result, increasing effect on flux performance of PVDF ENMs was observed.[140] In a recent study, covalently modified and fluorinated multi-walled carbon nanotubes (MWCNTs) (Fig. 9D) were incorporated to PH ENMs to construct 3D MD ENMs. The covalent modification enhanced the distribution of MWCNTs and the fluorination using FTES decreased the number of hydrogen and –OH groups of MWCNTs via hydrolysis and condensation, which enhanced their superhydrophobicity. These membranes, in DCMD exhibited about 60% higher water flux than the commercial PVDF membrane for the desalination 3.5 wt% NaCl solution.[141]

Several studies have been done on surface modification of ENMs for improving their performance in MD applications. In order to understand the correlation between nanofiber diameter and flux performance, Guo F et al. coated poly(1H,1H,2H,2H perfluorodecyl acrylate) (PPFDA) on poly(trimethylene hexamethylene terephthalamide) (PA6-3-T) ENMs using initiated chemical vapor deposition (iCVD) technique. The resultant membranes (fiber diameter ranging between 0.25 to 1.8 μm) were tested for salt rejection via AGMD process using 3.5 wt% NaCl solution. They observed increase in permeate flux from 2 to 11 kg m^{-2} h^{-1} for temperature differential of 25–40 °C between feed solution and the condenser plate. This was attributed to increase in liquid entry pressure (LEP$_W$) with increase of hydrophobicity and decrease of porosity (from 84 to 69%) of the membranes.[142] Shon et al. studied the effect of duration of CF$_4$ plasma surface modification on AGMD performance of PVDF ENMs. They found that the newly formed CF$_2$–CF$_2$ and CF$_3$ bonds imparted omniphobic property to the membrane's surface and lowered the surface energy, this improved the wetting resistance of membranes for liquids of low surface tension such as methanol, mineral oils and ethylene glycol.[143] Double-layered ENMs comprising hydrophobic active PH layer and different hydrophilic bottom layers such as PVA, Nylon-6, and PAN were tested for AGMD performance by YC Woo et al., CA of active layer was 140° and the CA of bottom ENM layers was less than 90°. The wettability of bottom hydrophilic ENMs enhanced the AGMD performance of dual layered ENMs.[144]

ENMs in reverse osmosis (RO)

The widely accepted pressure driven membrane technology for desalination is reverse osmosis (RO). The RO ENMs can remove the smallest particles such as monovalent ions like Cl$^-$ and Na$^+$.[145] The pore size of the RO ENMs varies between 0.1–1 nm.[146] Due to higher energy requirement of traditional thermal desalination processes, RO membranes are becoming increasingly important. Various nanomaterials have been extensively used to improve physico-chemical properties and filtration performance of RO desalination membranes, from traditional cellulose acetate membranes to present TFNC membranes. The TFNC membranes are of three layer structured membranes consisting the bottom supportive layer, middle porous layer and the top thin polyamide rejection layer formed by interfacial polymerization (Fig. 10).[147] From the past few years, there has been lot of research going on, to design high performance TFNC membranes. The scope of these membranes has been increasing exponentially in both domestic and industrial sectors due to their high productivity and high efficiency in removal of salts, minerals and various toxic chemicals from wastewater. The structural features, stability, and higher efficiency of TFNC membranes have made them a perfect option for the replacement of conventional RO membranes prepared by phase inversion technique.[148]

Few studies have been reported particularly on the fabrication and evaluation of the performance of RO ENMs. X. Wang et al. fabricated a robust RO TFNC ENM. They first prepared the
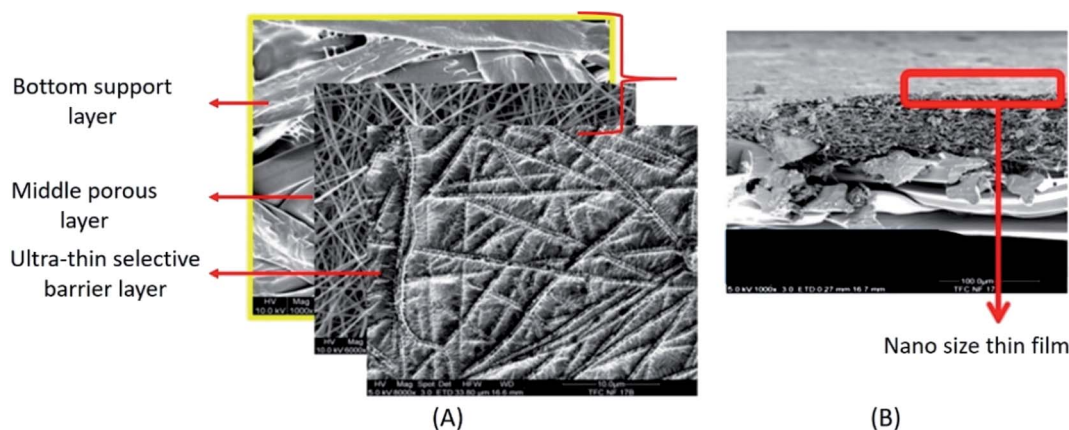

Fig. 10 An electrospun fabricated thin film nanocomposite membrane (TFNC); (A) SEM images showing different layers of a TFNC, (B) cross sectional SEM image of a TFNC, the region inside the red rectangle shows a few nanometres thick top selective layer formed by interfacial polymerization. Reproduced from ref. 147 with permission from Elsevier, copyright 2013.

porous layer of PAN ENM, and then on top of it a layer of cellulose nanofibers obtained from a biomass was casted to obtain a PAN/CNs substrate layer. On top of the substrate layer a thin polyamide (PA) layer was formed *via* interfacial polymerization using the monomers *m*-phenylene diamine and trimesoyl chloride to maintain better permeation flux and salt rejection. Their results showed the flux values around 41 L m^{-2} h^{-1} and salt rejection of above 95%, these values are almost closer to the performance of commercial XLE membrane that exhibits permeation flux between 40–70 L m^{-2} h^{-1} and salt rejection around 95%.[149] A cross-hatched composite nanofibrous TFNC ENM was developed by Kim *et al.*, they successfully fabricated PSf support layer by electrospinning and on top of it they fabricated a thin selective layer of PA by interfacial polymerization. The resultant ENMs were able to show better performance than the commercial traditional membranes by exhibiting permeation flux of 51 ± 2 L m^{-2} h^{-1} and salt rejection between 98–99%.[150] When fabricating TFNC RO ENMs, the importance has to be given to the effect of porous nanofibrous support layer on the formation of thin barrier layer by interfacial polymerization. The optimization of porosity and thickness, and enhancement of hydrophilicity of the barrier layers may be the effective research direction for the development of high-performance TFNC RO ENMs.

ENMs in forward osmosis (FO)

After RO, FO is the most commonly used techniques in a commercial way of desalination. The overall efficiency of FO process significantly varies with the type of membrane and draw solution used.[151] The performance of FO TFNC membranes is often inhibited by several problems, such as membrane fouling, concentration polarization, and reverse solute flux. Hence, the supportive layers of TFNC membrane need to be reengineered to make the desalination process cost effective. So far, PAN and cellulose acetate based blend ENMs, PES ENMs and nylon 6,6 based ENMs have been potentially used as supportive layers of TFNC FO desalination membranes due to their intrinsic open pore structure.[152]

For the first time, Hoover *et al.*[153] prepared the high performance trilayered TFNC membrane consisting of electrospun nanofiber support layer of polyethylene terephthalate, and a middle microporous polysulfone layer prepared by phase inversion method and the top polyamide layer formed by interfacial polymerization. Another high performance TFNC membrane for forward osmosis application was reported by M. Tian *et al.* They prepared thin film composite membrane using PVDF electrospun nanofiber as a substrate and on top of it an interfacially polymerized polyamide thin film layer with controlled pore size and surface roughness by varying the degree of cross linking.[152] They studied the FO performance of the resultant membranes and obtained 30.4 L m^{-2} h^{-1}, when the active layer faces the draw solution (1 M NaCl). Huang *et al.* prepared a TFNC FO membrane of electrospun PVDF nanofibrous substrate consisting top thin layer of nylon 6,6 formed by interfacial polymerization of adipoyl chloride and 1,6-hexane diamine. The resultant membrane was highly hydrophilic,

mechanically stable, and exhibited a lower swelling propensity than pristine nylon 6,6 ENM with excellent permeate flux.[154] Tian *et al.* successfully prepared a tiered structure support layer of polyetherimide (PEI) nanofibers incorporated with multi-walled carbon nanotubes as reinforcing agents and an ultra-thin polyamide-based selective top skin layer for FO desalination application.[155] Cross-linked PVA TFNC membranes have been reported for their efficient FO desalination performance, due to their ability to form a support layer with low tortuous pores and higher hydrophilicity. Compared to commercial FO membranes, these PVA membranes showed 7–8 times higher permeate flux.[156] E. L. Tian *et al.* prepared a TFNC FO membrane with the supportive layer of interpenetrating composite nanofibrous hydrophilic/hydrophobic network of hydrophilic polymer (PVA) and hydrophobic polymer (PET). They observed significant increase in the flux with increase of PVA content.[157] M. Shibuya *et al.* recently prepared a TFC-FO membrane, by using PVDF as core layer and CA as sheath layer. Their membrane exhibited better performance than a pure PVDF membrane, showing improved hydrophilicity, mechanical strength and permeate flux of 31.2 L m^{-2} h^{-1} for 0.5 M NaCl. However, TFFNCs consisting of an electrospun nanofiber supportive layers, with optimal porosity, mechanical stability and enhanced hydrophilicity with resistance to reverse solute flux have to be further explored to achieve significant progress in enhancing permeation flux and desalination performance of TFNC membranes.

ENMs for removal of dyes

The removal of various dye molecules from water using ENMs can be done through 2 different mechanisms. They are physical adsorption mechanisms and chemical adsorption mechanisms. Physical adsorption involves electrostatic interaction or intermolecular forces between the adsorbent and the dye molecules. Whereas, the chemical adsorption mainly depends upon the stable chemical interactions between the adsorbent and the dye molecules. The high specific surface area is the main requirement for efficient removal of dyes from water through physical and chemical adsorption mechanisms.[158] Due to the high specific surface area and high interconnected porosity, the ENMs can provide much better adsorption efficiency as compared to the traditional phase inversion membranes. The dyes removal efficiency of ENMs can be further enhanced either by functionalizing the membrane surface using adsorption materials with desired functional groups or by reducing the membrane surface by using reducing agents. However, the adsorption efficiency can be varied depending upon the environmental conditions such as pH and temperature. Depending upon the charge of the dye molecules in the solution, they can be classified as non-ionic and ionic dyes. The ionic dyes are again classified into anionic dyes and cationic dyes.

Common functional materials that have been incorporated to ENMs for removal of dyes from water are magnetic nanoparticles, graphene oxide (GO), PDA and β-cyclodextrin (β-CD). For example, an ENM of carbon nanofiber containing Fe_3O_4 magnetic nanoparticles (CNFs/Fe_3O_4 NPs) was developed by Si

et al. via combination of electrospinning and *in situ* polymerization involving polybenzoxazine precursors. The resultant ENMs exhibited high specific surface area and porosity of 1885 m² g⁻¹ and 2.325 cm³ g⁻¹ respectively with excellent organic dyes removal from water and magnetic separation efficiency.[159] PES/PEI ENM system rich with amino and imino functionalities was developed by Min *et al.* for the efficient adsorptive removal of dye molecules such as Sunset Yellow FCF, Fast Green FCF and also Amaranth. In another study, Q. Wang *et al.* fabricated 4 different kinds of sodium alginate (SA) based ENMs (SA ENMs) for cationic dye methylene blue (MB) removal from water. Among them one ENM fabricated by without any crosslinking and the other 3 by using 3 different crosslinking agents such as calcium chloride (CaCl₂), glutaraldehyde vapour (GA) and trifluoroacetic acid (TFA). The non-cross-linked SA and CaCl₂ cross-linked SA ENMs showed almost same specific surface area values with 13.97 and 13.56 m² g⁻¹ respectively, while the surface area increased to 15.2656 m² g⁻¹ for TFA cross-linked ENM and decreased to 11.86 m² g⁻¹ for GA cross-linked ENM. The maximum MB dye adsorption capacity of 2230 mg g⁻¹ was obtained for CaCl₂ cross-linked SA ENMs, which was much greater than the adsorption ability of all other previously reported alginate and other material based ENMs.[160] The β-cyclodextrin (β-CD) based ENMs for removal of MB was successfully fabricated by R. Zhao *et al.* by electrospinning a solution containing appropriate mixture of β-CD, PAA and citric acid followed by thermal crosslinking. Due to the higher content of β-CD and due to the presence of –COOH groups the ENMs showed excellent MB adsorption capacity of 826 mg g⁻¹, which was much higher than that of most of the β-CD based adsorbents.[161] An ENMs of PLLA coated with *p*-toluenesulfonic acid doped polyaniline (*p*-TSA-PANI/PLLA ENMs) was developed by Yomen Atassi *et al.* for the removal of methyl orange (MO) anionic dye from water. The *p*-TSA-PANI/PLLA ENMs exhibited specific surface area of 8.3 m² g⁻¹. Under sorption conditions such as temperature of 25 °C, pH = 6, dye concentration 550 ppm, and contact time of 24 h, the membranes exhibited adsorption capacity of 377 mg g⁻¹, which was comparable to the values of excellent adsorbents.[162] W. Jang *et al.* successfully dispersed an exfoliated GO modified with cetyltrimethylammonium chloride (cGO) in PAN solution and obtained cGO-PAN ENMs by electrospinning for the removal of MB and methyl red (MR) from water. The GO content was varied upto 30 wt% without any problem to achieve maximum adsorption efficiency. The higher GO content with various oxygenated functional groups contributed towards better dyes removal efficiency, *via* various interactions such as electrostatic, hydrogen bonding, and π–π interactions. Advantageously, the ENMs as the carriers of these various functional materials, not only avoid the agglomeration of these materials in dye solution but also further increase the specific surface area for dyes adsorption.[163]

ENMs for removal of heavy metals

In consideration of health and environmental safety, the effective removal of toxic metal ions from contaminated water has found to be very important. There are several techniques to remove toxic metal ions from water, such as chemical precipitation, electrodialytic separation, adsorption based membrane filtration, and solvent extraction. Compared to these methods, the adsorption method is simple, cost effective and easy to carry out. The better removal heavy metals by the adsorbents depends upon the surface area, porosity, selectivity, adsorption capacity and ability to withstand degradation at higher temperature and radiations.[80] Intake of water contaminated with any kind of toxic heavy metal such as chromium, fluorine, mercury, cadmium, lead, arsenic is very harmful to human health. For example, consumption of water contaminated with arsenic (As III & As V) induces disorders to nervous, circulatory and digestive system and also to skin. Toxic effect of Cr(VI) causes cancer and mutation in living organisms and intake of drinking water containing fluoride concentration more than 1 mg L⁻¹ also causes skeletal disorders (dental and skeletal fluorosis) (Fig. 11).

Recently, ENMs have gained tremendous attention for removal of toxic metal ions from contaminated water. Their high surface volume for chemical and physical interactions and interconnected porosity can allow more amounts of target compounds to interact with the nanofibrous surface. The polymers such as cellulose acetate, chitosan, poly acrylic acid, silk fibroin have greater metal ion adsorption efficiency. Chitosan has been used as a very common adsorbent due to its strong interaction with metal ions through its amine groups.[166] Chitosan is more effective in its electrospun nanofibrous form for heavy metal ions removal than in its other forms such as films, beads, gel or sponge, or nanoparticles. Min *et al.* fabricated chitosan ENMs (CS-ENMs) for the removal of As(v) from water.[167] They observed maximum adsorption capacity of 30.8 mg g⁻¹ at solution pH of 3.4 in 0.5 h. This was the highest
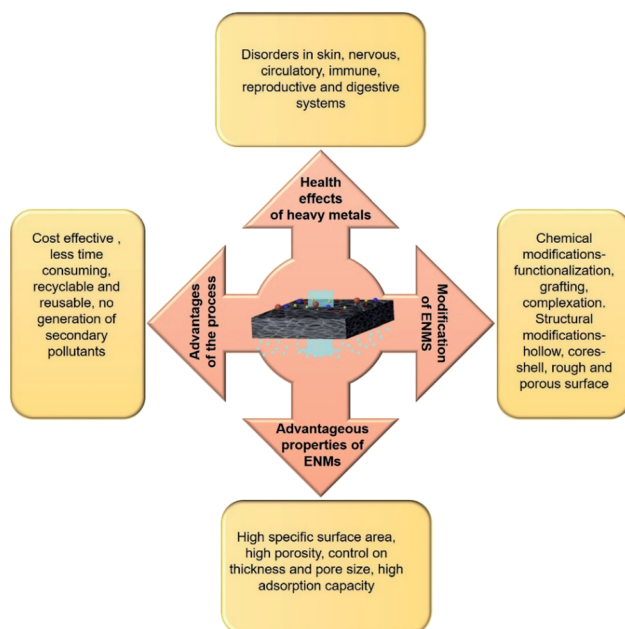

Fig. 11 Schematic representation of adsorptive removal of heavy metal ions *via* an ideal polymeric ENM showing negative impacts of heavy metals on human health, different ways of modification of ENMs and advantageous properties of an ideal ENM for heavy metal removal from aqueous system.

performance reported for chitosan based adsorbents for removal of As(v) from water. Sharma *et al.* investigated the efficiency of electrospun cerium(III)-chitosan/PVA composite ENMs for removal of As(III) ions from water, they obtained adsorption capacity of 18 mg g^{-1} and these ENMs purified water below the prescribed limit of WHO/EPA up to 1500 μg L^{-1}. Moreover, Ce-CS/PVA composite ENMs were nontoxic, which made them suitable for water purification application (Fig. 12A).[164] In order to enhance the heavy metal removal ability of chitosan ENMs, Ma *et al.* fabricated CS-poly(glycidyl methacrylate) PGMA-PEI ENMs rich with amine functionality and investigated their efficiency for the adsorptive removal of heavy metal ions such as Cr(vi), Cu(ii) and Co(ii) from aqueous system. Their results of adsorption studies revealed that the optimal pH was 2.0, 4.0 and 6.0 for the removal of Cr(vi), Cu(ii) and Co(ii), respectively. The highest adsorption capacity of Cr(vi), Cu(ii) and Co(ii) was 138.96, 69.27 and 68.31 mg g^{-1}, respectively[168] (Fig. 13).

The electrospun chitosan/hydroxyapatite (CS/HAp) composite ENMs were tested by Aliabadi *et al.* for removal of heavy metals such as lead, cobalt and nickel ions from water.

Their membranes showed greater adsorption efficiency for Pb, Cd and Ni ions in the order of (296.7 mg g^{-1}) > (213.8 mg g^{-1}) > (180.2 mg g^{-1}) respectively.[169] Lakhdhar *et al.* used ENMs of (PEO)/chitosan to remove Cu(ii) ions from aqueous solutions, their membranes exhibited adsorption capacity of about 94.7% for 75 mg of (PEO)/chitosan nanofibers in 3:20 hours, at the temperature of 55.7 °C and the pH 5.5, with initial Cu(ii) ions concentration of 100 ppm.[170]

The ENMs of polymers other than chitosan have also shown better efficiency for the removal of heavy metals from aqueous system. For example, Quan Feng *et al.* fabricated AOPAN/RC blend ENMs and studied their efficiency for the removal of heavy metal ions such as Fe(iii), Cu(ii) and Cd(ii) ions separately from their aqueous solutions. The adsorption capacities of AOPAN/RC blend ENMs (at 25 °C) for Fe(iii), Cu(ii) and Cd(ii) were 7.47, 4.26 and 1.13 mmol g^{-1}, respectively. Their adsorption results revealed that the AOPAN/RC membrane can adsorb the heavy metal ions Fe(iii), Cu(ii) and Cd(ii) from water effectively, due to the synergistic effect between amidoxime and hydroxyl functionalities towards coordination/chelation of
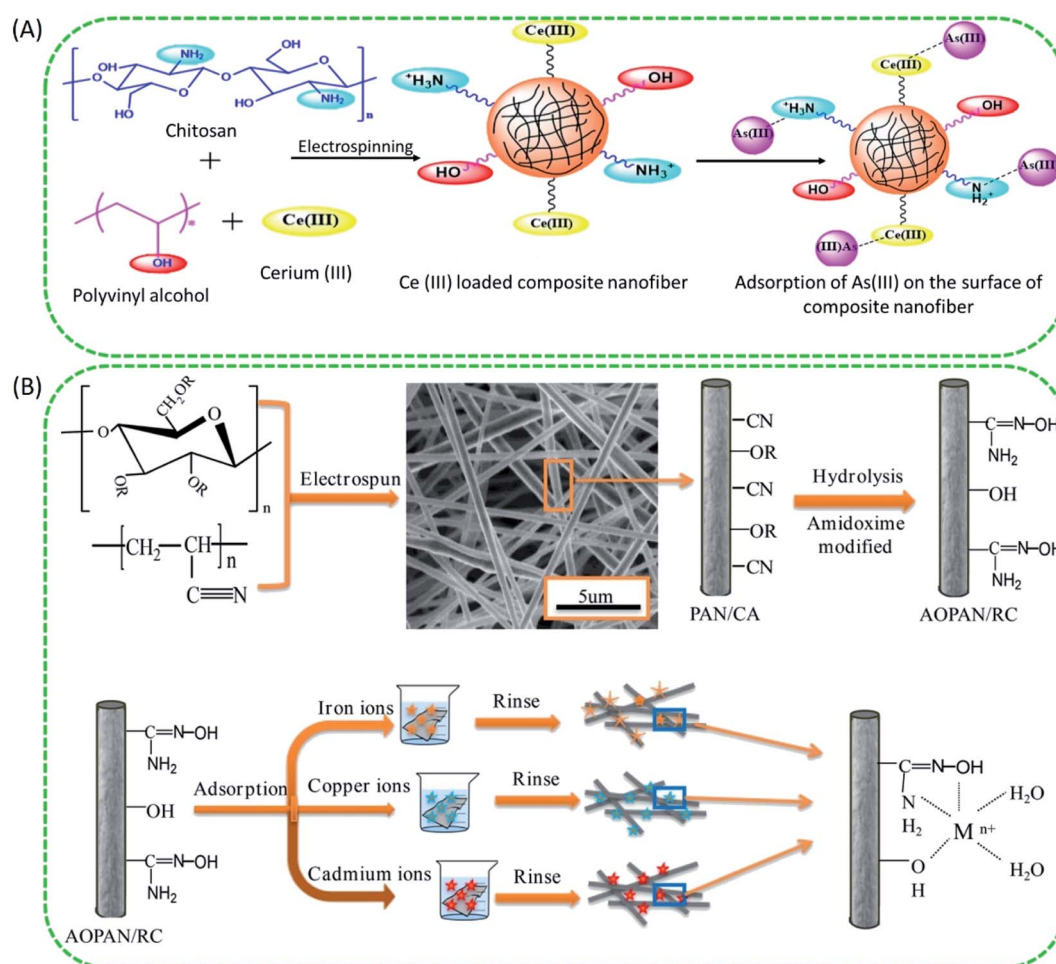

Fig. 12 (A) Probable modified reaction mechanism of As(III) adsorption on cerium(III)-CS/PVA composite nanofiber.[164] Reproduced from ref. 164 with permission from Royal Society of Chemistry, copyright 2014. (B) Schematic representation of the preparation and evaluation of amidoxime polyacrylonitrile/regenerate cellulose (AOPAN/RC) blend ENMs for adsorptive removal of heavy metal ions from aqueous system.[165] Reproduced from ref. 165 with permission from Elsevier, copyright 2018.
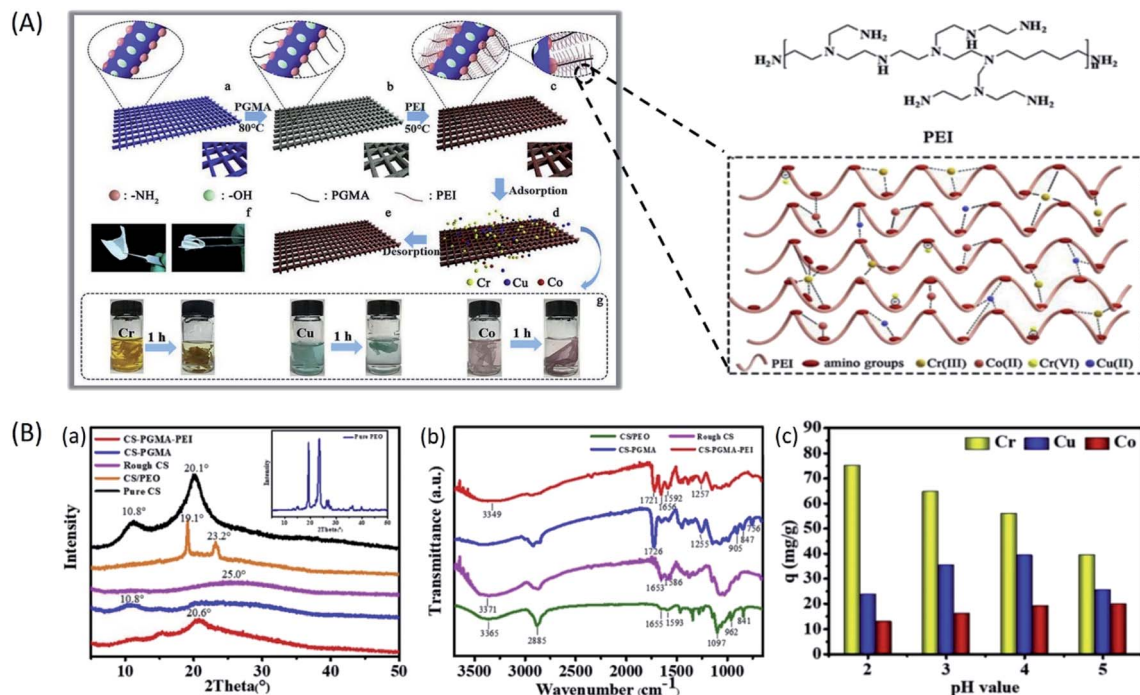
Fig. 13 (A) Schematic illustration of the preparation of the CS-PGMA-PEI ENM and its application in removal of heavy metal ions from water. (B) Chemical characterization and performance evaluation of CS-PGMA-PEI ENM; (a) XRD patterns. (b) ATR-FTIR spectra. (c) Effect of pH on competitive adsorption among Cr(VI), Cu(II), and Co(II) ions.[168] Reproduced from ref. 168 with permission from Elsevier, copyright 2019.

heavy metal ions[165] (Fig. 12B). Hallaji *et al.* fabricated PVA/ZnO based ENM adsorbents and studied their efficiency for the removal of metal ions such as Cu(II), Ni(II) and U(VI), ions from water, their results indicated that the adsorption capacity values of 370.86, 162.48 and 94.43 mg g^{-1} for sorption of U(VI), Cu(II) and Ni(II) ions, respectively, under the experimental conditions of contact duration 6 h, adsorbent concentration 1 g L^{-1}, temperature 45 °C, and pH 5.0. In another study, Keshtkar *et al.* prepared both an ENMs and the solution casted homogeneous membrane of PVA/tetraethyl orthosilicate (TEOS)/amino propyl triethoxysilane (APTES), to remove uranium from water and obtained adsorption capacity of 75.9 and 13.7 mg g^{-1} for electrospun and solution casted membranes respectively.[171] Alumina nanofibers prepared by casting a solution containing PVP and aluminium acetate were able to remove 6.8 mg g^{-1} Cr(VI) and 1.2 mg g^{-1} of fluoride ions from water at pH range of 5–7.[80] In another study, to remove Cr from water, Zhou *et al.* fabricated a composite nanofiber of PAN/ferrous chloride (FeCl$_2$) by electrospinning. They obtained excellent Cr adsorption efficiency of about 108 mg Cr per g FeCl$_2$.[172] Wu *et al.* prepared an electrospun polypyrrole (PPy)/PES nanofiber membrane to separate silver ions from water. They found maximum adsorption efficiency of about 35.7 mg of Ag(I) ions per gram of PES/PPy membrane.[173] Although several progresses have been made for the efficient adsorptive removal of heavy metal ions from water using ENMs adsorption technology, there are still a different varieties of contaminants in the practical wastewater system. That may lead to fouling of nanofiber membranes, consequently leading to failure of adsorption active sites of nanofibers. Hence, it is important to conduct

more studies on the development of very efficient adsorbents with properties such as high robustness to fouling, biodegradability, reusability, high specific surface area and porosity *etc.*, for large scale practical wastewater treatment applications.

ENMs for oil–water separation

Oil spill accidents and industrial oily wastewaters have led to serious environmental pollution and great loss of energy, threatening both the lives of human beings and aquatic animals. Therefore, efficient control of oil/water pollution with new techniques and materials is necessary for healthy living and also to protect ecosystem. Some materials in nature like lotus leaf or colocasia leaf which show excellent water repellent property. Inspired by such materials in nature, scientists have developed varieties of special materials which are selectively wettable to oil and water for different applications. Several techniques have been demonstrated to separate oil and water such as, ultrasonic separation, centrifugation, skimming, coagulation–flocculation techniques, biological treatment, and air flotation in a conventional way. However, these separation techniques involve physico-chemical or biological approaches generating secondary pollutants, and exhibiting problem of low efficiency of separation, and poor retention and reusability. Therefore, to achieve efficient oil–water separation, efficient super-hydrophobic (water contact angle >150°) and super-hydrophilic (water contact angle <10°) materials have been developed by various physical and chemical methods such as chemical vapour deposition, hydrothermal synthesis, colloidal assembly, plasma treatment and chemical etching. However, some of these techniques are still not suitable practically,
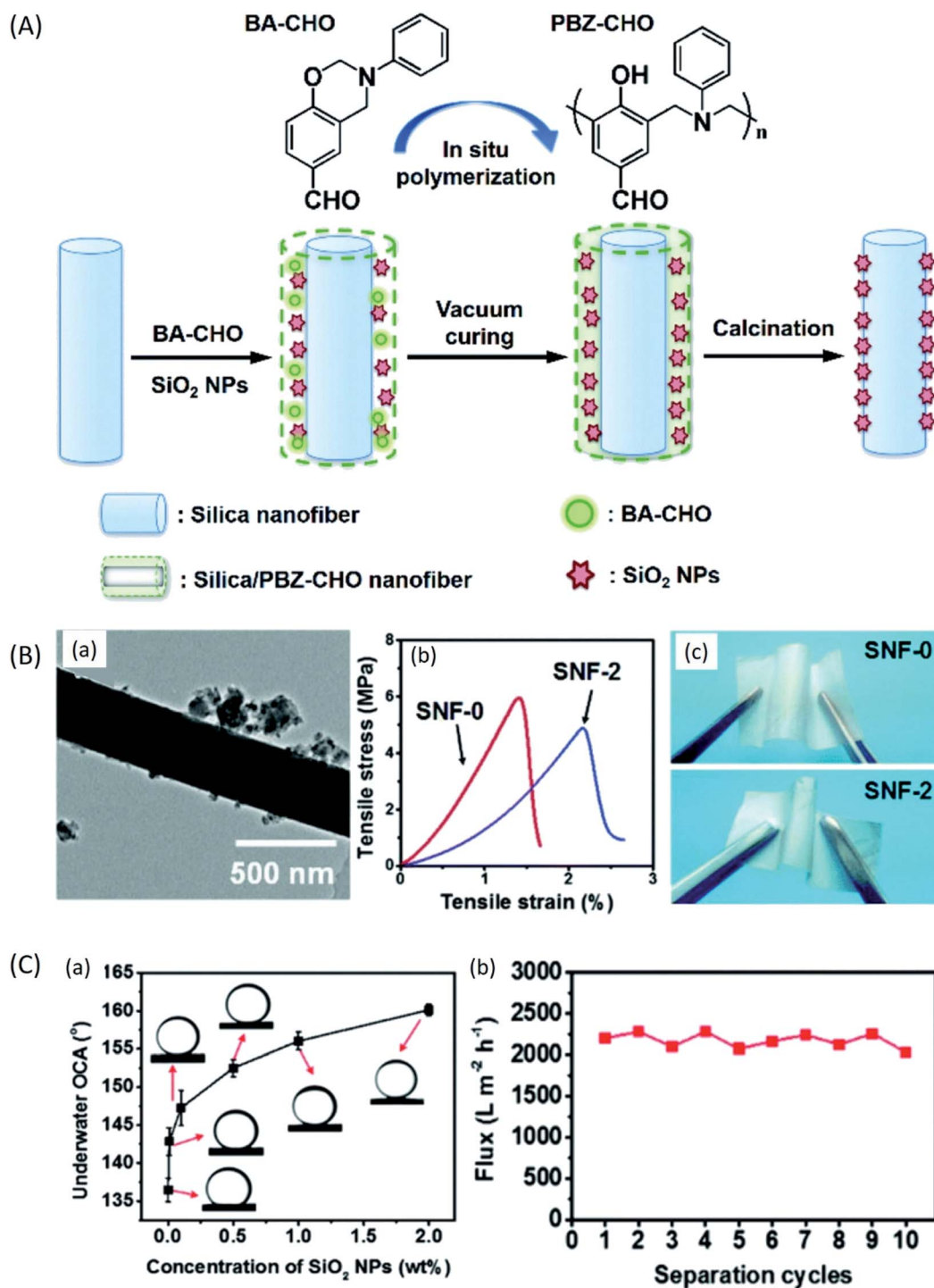
Fig. 14 Silica/PBZ–CHO ENMs for oil/water microemulsion separation; (A) schematic of synthesis of hierarchical porous Silica/PBZ–CHO ENMs, (B) morphological and mechanical characterization; (a) TEM image of Silica/PBZ–CHO ENM doped with 2 wt% silica, (b) tensile stress–strain curves of Silica/PBZ–CHO ENMs without silica and with 2 wt% silica, (c) digital images show the robust flexibility of Silica/PBZ–CHO ENMs without silica and with 2 wt% silica, (C) wettability and permeability studies: (a) underwater oil contact angle (OCA(°)) of Silica/PBZ–CHO ENMs, (b) changes in separation flux with increasing number of cycles using Silica/PBZ–CHO ENMs.[174] Reproduced from ref. 174 with permission from The Royal Society of Chemistry, copyright 2014.

because of poor stability, selectivity and high energy requirements.

From the past few years, membrane separation has been regarded as a promising approach for oil/water separation, due to its simplicity and cost-effectiveness. However, several drawbacks need to be resolved especially in micro and ultra-filtration based oil–water separations, due to reduced permeation flux intensive fouling, and less reusability. In order to counteract
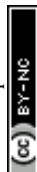
these problems, polymeric ENMs are the promising materials with suitable properties such as controllable porosity, surface chemistry and mechanical properties that can eliminate membrane fouling, formation of secondary pollutants, and process cost with reusability. The ENMs of polymers such as polystyrene (PS), polyacrylonitrile (PAN), poly vinylidene fluoride (PVDF) and poly methyl methacrylate (PMMA) have been successfully demonstrated for oil–water separation applications. In order to separate oil and water using low pressure technique, Tang et al. developed the membranes with wide range of pH stability, with good separation efficiency and water repellency using ENMs of poly (m-phenylene isophthalamide) (PMIA) as super-hydrophilic layer and fluorinated poly benzoxazine (F-PBZ) loaded with SiO_2 nanoparticles as super-hydrophobic layer. Their ENMs exhibited the permeate flux of 3311 L m^{-2} h^{-1}, which was significantly greater than that of commercial ultrafiltration (UF) membranes, which usually exhibit the permeate flux of 300 L m^{-2} h^{-1}.[176] EF Ahmed et al.

prepared a poly vinylidene fluoride-co-hexafluoro-propylene (PVDF-HFP) nano fibrous scaffold by electrospinning. The resultant membranes were super hydrophilic and super-oleophobic under water, with an oil/water separation efficiency about 99.98%.[177] To enhance the gravity driven flux of PVDF-HFP ENMs, S.M. Seyed Shahabadi et al. coated carbon black nanoparticles onto PVDF-HFP ENMs by electrospraying, after carbon black nanoparticles coating, they observed super-hydrophobicity in PVDF-HFP ENMs with CA value of 160.8°, 7.0° with great enhancement in gravity-driven flux (1275–2163 L m^{-2} h^{-1}) for the tested non-aqueous solvents. Yang S et al. fabricated silica/polybenzoxazine (PBZ-CHO) ENMs doped with different concentrations of silica (0.5 wt% to 2 wt%) for efficient dee-mulsification of oil in water micro-emulsions. Their membranes exhibited underwater superoleophobicity with excellent mechanical, thermal and antifouling properties and exhibited separation flux of 2237 L m^{-2} h^{-1}; under gravity driven separation, which was higher than that of commercial
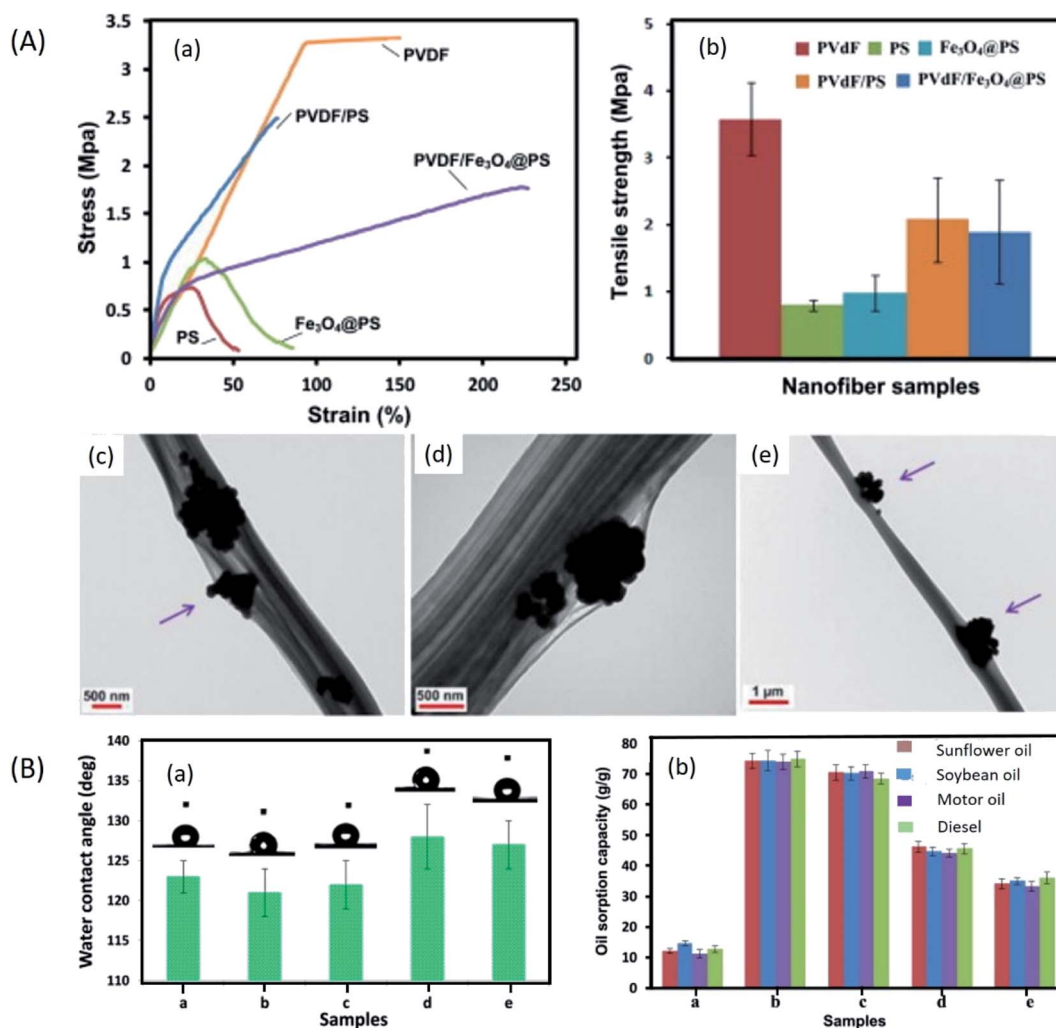

Fig. 15 Two-nozzle electrospun fabricated PS/PVDF/Iron oxide ENMs for oil–water separation; (A) mechanical and morphological characterization of PS/PVDF/Iron oxide ENMs; (a) stress–strain curves, (b) tensile strength, (c and d) TEM images, (B) wettability and oil–water separation study of PS/PVDF/Fe$_3$O$_4$ ENMs; (a) water contact angle measurement, (b) oil adsorption capacity of PS/PVDF/Fe$_3$O$_4$ ENMs for different oils.[175] Reproduced from ref. 175 with permission from Elsevier, copyright 2015.

pressure driven separation membranes (Fig. 14).[174] A magnetic composite ENM of PS-Iron oxide (Fe$_3$O$_4$)/(PVDF) nanofibers was developed by Jing Z. *et al.* The PS and PVDF both imparted oleophilicity and hydrophobicity with enhanced mechanical stability to the ENM. Fe$_3$O$_4$ nanoparticles enabled easy recovery of ENM after adsorption of oil from water, the oil sorption capacity was about 35–46 g g^{-1} (Fig. 15).[175] Raza A. *et al.* successfully demonstrated an *in situ* cross-linked polyethylene glycol diacrylate nanofibers supported on polyacrylonitrile/ polyethylene glycol nanofibrous (*x*-PEGDA@PG NF) membranes for gravity driven separation of immiscible mixtures of oil and water and oil in water micro emulsions. Their membranes (pore size 1.5–2.6 µm) showed a very high permeate flux of 10 975 L m^{-2} h^{-1}, with excellent antifouling properties and high viscous oil separation efficiencies.[178] Po-Yu *et al.* used polystyrene and a co-solvent system consisting a solvent chlorobenzene and a nonsolvent DMSO for

electrospinning, the resultant nanofiber were highly porous with super hydrophobic surface and exhibited ultra-high oil adsorption ability of 600–800 g per min per gram (g) of sorbent.[179] Luo *et al.* prepared a high flux ENM with switchable permeability to oil and water for gravity based oil–water separation application. They prepared smart ENM of poly (methyl methacrylate)-*block*-poly(4-vinylpyridine) (PMMA-*b*-P4VP), a pH sensitive copolymer. As such the ENM was permeable only to oil, after dipping the membrane into an aqueous acidic medium of pH 3, the permeability changed from oil to water.[180] W. Ma *et al.* fabricated a fluorine free polyimide (PI) based ENM coated with PBZ containing silica nanoparticles. Their membranes presented oil/water separation efficiency above 99% and high permeate flux about 4798 L m^{-2} h^{-1} with excellent reusability.[181] Very recently, Y. YI *et al.* grafted the surface of plasma-treated polystyrene/polyacrylonitrile (PS/PAN) electrospun membranes with acrylic acid. They obtained a very
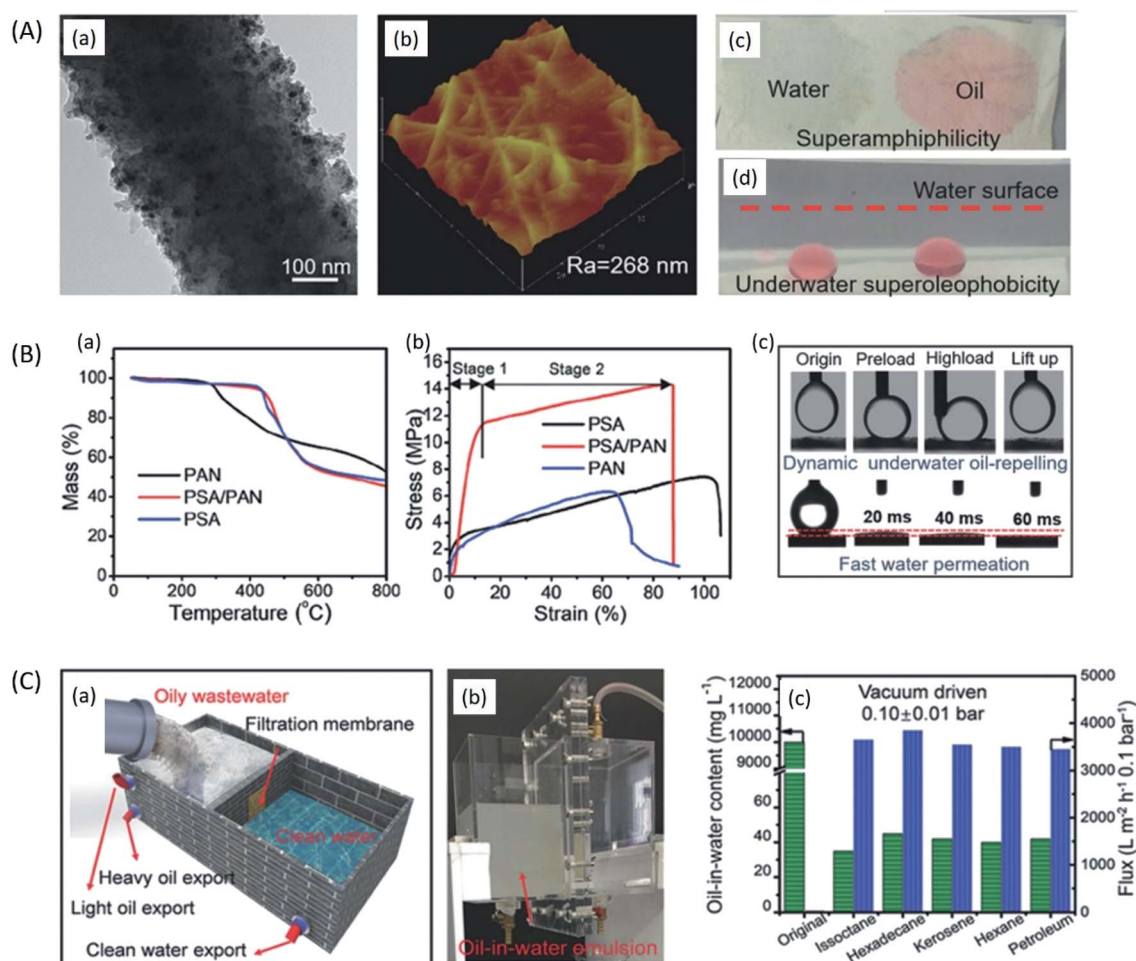

Fig. 16 Calcinable hierarchical titanium dioxide (TiO$_2$)-polysulfonamide (PSA)/PAN ENMs for long term oil/water separation application; (A) morphology and wettability characterization; (a) TEM and (b) AFM images of the hierarchical TiO$_2$-0.4@PSA/PAN ENM. (c) Water and oil droplets dyed with Sudan red G on the TiO$_2$-0.4@PSA/PAN ENM in air. (d) Digital image of underwater oil droplets (3 µL) on the surface of TiO$_2$-0.4@PSA/ PAN ENM. (B) Thermal, mechanical and wettability properties of hierarchical TiO$_2$-PSA/PAN ENMs; (a) TGA, (b) stress−strain curves, (c) digital images of underwater oil-repelling and dynamic water permeation measurements on the surface of TiO$_2$-0.4@PSA/PAN ENM. (C) Separation devices and separation efficiency; (a) schematic diagram showing the separation set up in real application, (b) digital image showing the cus- tom-made separation device in operation, (c) the pure water flux and the separation performance for the various oil-in-water emulsions using TiO$_2$-0.4@PSA/PAN ENM. Reproduced from ref. 183 with permission from Wiley-VCH GmbH, Weinheim, copyright 2018.

high permeate flux of 57 509 L m^{-2} h^{-1} for layered oil/water mixtures.[182] Applications of metallic glass coatings for oil/water separation ENMs were also reported. J.P. Chu *et al.* coated PAN ENMs with Zr-based thin film metallic glass (TFMG) (Zr$_{53}$Cu$_{26}$Al$_{16}$Ni$_5$) *via* magnetron sputtering. The coating provided protection from chemicals high temperature and irreversible internal fouling. They also studied the effect of SDS surfactant on oil/water separation efficiency. Depending upon the concentration of SDS, the membranes showed separation efficiency of 95% to 100%. For long term oil/water separation application, Z. Zhu *et al.* fabricated PSA/PAN ENM by emulsion electrospinning, followed by hydrothermal infusion of TiO$_2$ nanoparticles. Their membrane displayed outstanding thermal resistance in air (upto 400 °C) and strong chemical resistance (at the pH range of 1 to 13) and mechanical robustness. As a result, the membrane enabled easy removal of chemical foulants from its surface after the oil/water separation by calcination without reducing its separation efficiency. Their membrane exhibited water flux of 3000 L m^{-2} h^{-1} and oil rejection efficiency of 99.6% for separation of various oil-in-water emulsions[183] (Fig. 16). Although, electrospinning technology has made tremendous progress in oil-water separation research, there are only few studies reported about (i) recovery and recyclability of the adsorbents, (ii) ENMs of ultra-high adsorption or gravity driven separation ability with robustness to fouling, (iii) materials for switchable oil–water permeability and (iv) materials for selective separation of oils from complex oil–water mixtures. Therefore, for further exploration of these areas, novel nanofiber materials for oil–water separation need to be developed.

Conclusion and outlook

Electrospinning is a prevailing technology to produce advanced nanofibrous materials for various applications. The water purification performance of ENMs depends on the properties such as high surface area, high porosity, high surface roughness, and surface chemistry (hydrophobicity/hydrophilicity). These properties are often altered by the influence of both limiting factors of electrospinning and the chosen functional materials. This provides a promising platform to tune the properties such as surface roughness, porosity, and thickness of ENMs. Hence, firstly in this review, we explored the influence of limiting factors on morphology of polymeric nanofibers. Secondly, we discussed about the recent developments in electrospinning, enabling faster production of nanofibers with different morphology, including their alignment in a required direction. Finally, we briefly discussed the recent and last progresses in performance and potential of ENMs to expel pollutants from aqueous system. The ENMs have been successfully applied for different membrane separation areas, such as MF, RO, FO, MD, heavy metal removal, and oil/water separation. Unquestionably, ENMs have established a promising platform for water treatment, where (i) fabricating ENMs by doping a polymer solution with nanomaterials from ceramics, metals/metal oxide and carbon, and (ii) treating the surface of ENMs by functionalization, (iii) developing a top selective layer by interfacial polymerization for TFNC, and (iv) grafting and chemical etching strategies have well extended the potential of ENMs. However, more research progress is needed in the areas of (i) using biodegradable polymers with negative surface charge to enhance fouling resistance of microfiltration ENMs, (ii) developing a superhydrophobic microporous ENMs with high porosity for MD application, (iii) developing a reusable and fouling resistant high specific surface area ENMs with ability to adsorb more than one type of heavy metal ions, and (iv) surface coating of ENMs by various sputtering/coating techniques for tuning their surface wettability for high flux gravity driven oil/water separation application. These are some of the emerging promising strategies which will further extend the potential of ENMs in different areas of water purification. The design, development and implementation of cost-effective and high performance ENMs in membrane technology *via* innovative electrospinning technologies is anticipated to contribute a lot in addressing the world's fresh water scarcity and pollution problems in the near future.

## Conflicts of interest

There are no conflicts to declare.

Acknowledgements

Notes and references

1 M. Imran, S. Haider, K. Ahmad, A. Mahmood and W. A. Al-masry, *Arabian J. Chem.*, 2017, **10**, S1067–S1072.

2 K. C. K. Cheng, M. A. Bedolla-Pantoja, Y.-K. Kim, J. V. Gregory, F. Xie, A. de France, C. Hussal, K. Sun, N. L. Abbott and J. Lahann, *Science*, 2018, **362**, 804–808.

3 U. Tritschler, J. Gwyther, R. L. Harniman, G. R. Whittell, M. A. Winnik and I. Manners, *Macromolecules*, 2018, **51**, 5101–5113.

4 C. Shen, C.-P. Wang, M. Sanghadasa and L. Lin, *RSC Adv.*, 2017, **7**, 11724–11731.

5 L. Xia, J.-g. Ju, W. Xu, C.-k. Ding and B.-w. Cheng, *Mater. Des.*, 2016, **96**, 439–445.

6 X. Hu, X. Zhang, X. Shen, H. Li, O. Takai and N. Saito, *Plasma Chem. Plasma Process.*, 2014, **34**, 1129–1139.

7 R. Vasireddi, J. Kruse, M. Vakili, S. Kulkarni, T. F. Keller, D. C. F. Monteiro and M. Trebbin, *Sci. Rep.*, 2019, **9**, 14297.

8 A. Suzuki, T. Mikuni and T. Hasegawa, *J. Appl. Polym. Sci.*, 2014, **131**.

9 Y. E. Kiyak, *Electronic Journal of Textile Technologies*, 2014, **8**(3), 49–60.

10 S. Ramakrishna, K. Fujihara, W.-E. Teo, T. Yong, Z. Ma and R. Ramaseshan, *Mater. Today*, 2006, **9**, 40–50.

11 S. Thenmozhi, N. Dharmaraj, K. Kadirvelu and H. Y. Kim, *Mater. Sci. Eng., B*, 2017, **217**, 36–48.

12 W. E. Teo and S. Ramakrishna, *Nanotechnology*, 2006, **17**, R89–R106.

13 J. Huang and T. You, *Electrospun Nanofibers: From Rational Design, Fabrication to Electrochemical Sensing Applications*, 2013.

14 L. Hou, N. Wang, J. Wu, Z. Cui, L. Jiang and Y. Zhao, *Adv. Funct. Mater.*, 2018, **28**, 1801114.

15 Y. Liao, C.-H. Loh, M. Tian, R. Wang and A. G. Fane, *Prog. Polym. Sci.*, 2017, **77**, 1–118.

16 Z. Li and C. Wang, in *One-Dimensional nanostructures: Electrospinning Technique and Unique Nanofibers*, Springer Berlin Heidelberg, Berlin, Heidelberg, 2013, pp. 15–28, DOI: 10.1007/978-3-642-36427-3_2.

17 V. Pillay, C. Dott, Y. E. Choonara, C. Tyagi, L. Tomar, P. Kumar, L. C. du Toit and V. M. K. Ndesendo, *J. Nanomater.*, 2013, **2013**, 22.

18 T. Senthil and S. Anandhan, *J. Elastomers Plast.*, 2015, **47**, 327–346.

19 A. H. Hekmati, N. Khenoussi, H. Nouali, J. Patarin and J.-Y. Drean, *Text. Res. J.*, 2014, **84**, 2045–2055.

20 A. R. Noorpoor, A. Sadighzadeh and A. Anvari, *Int. J. Environ. Res.*, 2014, **8**, 421–426.

21 K. Matabola and R. Moutloali, *The influence of electrospinning parameters on the morphology and diameter of poly(vinyledene fluoride) nanofibers—Effect of sodium chloride*, 2013.

22 H. Shao, J. Fang, H. Wang and T. Lin, *RSC Adv.*, 2015, **5**, 14345–14350.

23 M. Dasdemir, M. Topalbekiroglu and A. Demir, *J. Appl. Polym. Sci.*, 2013, **127**, 1901–1908.

24 M. M. Munir, A. Nuryantini, K. Khairurrijal, M. Abdullah, F. Iskandar and K. Okuyama, *Preparation of Polyacrylonitrile Nanofibers with Controlled Morphology Using a Constant-Current Electrospinning System for Filter Applications*, 2013.

25 L. Li, Z. Jiang, J. Xu and T. Fang, *J. Appl. Polym. Sci.*, 2014, **131**, 40304.

26 H. Maleki, A. A. Gharehaghaji, G. Criscenti, L. Moroni and P. J. Dijkstra, *J. Appl. Polym. Sci.*, 2015, **132**(5), 41388.

27 N. A. Abdullah, K. Ahmad Sekak and M. R. Ahmad, *Adv. Mater. Res.*, 2016, **1134**, 203–208.

28 B. Cramariuc, R. Cramariuc, R. Scarlet, L. R. Manea, I. G. Lupu and O. Cramariuc, *J. Electrost.*, 2013, **71**, 189–198.

29 M. Mohammad Ali Zadeh, M. Keyanpour-Rad and T. Ebadzadeh, *Ceram. Int.*, 2014, **40**, 5461–5466.

30 J. Lasprilla-Botero, M. Álvarez-Láinez and J. M. Lagaron, *Mater. Today Commun.*, 2018, **14**, 1–9.

31 K. P. Matabola and R. M. Moutloali, *J. Mater. Sci.*, 2013, **48**, 5475–5482.

32 X. L. Cai, T. T. Jiang, C. M. Qiao, B. W. Cheng and W. M. Kang, *Appl. Mech. Mater.*, 2014, **633–634**, 11–14.

33 X. Lin, Y. Li, Z. Chen, C. Zhang, X. Luo, X. Du and Y. Huang, *Chem. Eng. J.*, 2013, **215–216**, 709–720.

34 A. Haider, S. Haider and I.-K. Kang, *Arabian J. Chem.*, 2018, **11**, 1165–1188.

35 S. S. Esnaashari, S. Rezaei, E. Mirzaei, H. Afshari, S. M. Rezayat and R. Faridi-Majidi, *Int. J. Biol. Macromol.*, 2014, **70**, 50–56.

36 X. Cao, M. Huang, B. Ding, J. Yu and G. Sun, *Desalination*, 2013, **316**, 120–126.

37 A. H. Hekmati, A. Rashidi, R. Ghazisaeidi and J.-Y. Drean, *Text. Res. J.*, 2013, **83**, 1452–1466.

38 R. T. Oğulata and H. İ. İçoğlu, *J. Text. Inst.*, 2015, **106**, 57–66.

39 J. Zhao, N. Si, L. Xu, X. Tang, Y. Song and Z. Sun, *Mater. Chem. Phys.*, 2016, **170**, 294–302.

40 X. Li Cai, T. Ting Jiang, C. Mei Qiao, B. Wen Cheng and W. Min Kang, *Effect of Electrospinning Process on Electrospun Chlorinated Polyvinyl Chloride (CPVC) Nanofibers*, 2014.

41 S. Singh, V. Singh, V. M. and V. V. Bhanu Prasad, *ZrO_2 fibers obtained from the halide free synthesis of non-beaded PVA/Zr n-propoxide electrospun fibrous composites*, 2013.

42 R. Ghelich, M. Keyanpour Rad and A. Mansoor Youzbashi, *Nanofibers*, 2015, **10**, 12–19.

43 R. Ghelich, M. K. Rad and A. A. Youzbashi, *J. Eng. Fibers Fabr.*, 2015, **10**, 155892501501000102.

44 J. Pelipenko, J. Kristl, B. Janković, S. Baumgartner and P. Kocbek, *Int. J. Pharm.*, 2013, **456**, 125–134.

45 B. De Schoenmaker, L. Van der Schueren, R. Zugle, A. Goethals, P. Westbroek, P. Kiekens, T. Nyokong and K. De Clerck, *J. Mater. Sci.*, 2013, **48**, 1746–1754.

46 P. Moutsatsou, K. Coopman, M. B. Smith and S. Georgiadou, *Polymer*, 2015, **77**, 143–151.

47 H. Fashandi and M. Karimi, *Ind. Eng. Chem. Res.*, 2014, **53**, 235–245.

48 S. S. Ray, S.-S. Chen, C.-W. Li, N. C. Nguyen and H. T. Nguyen, *RSC Adv.*, 2016, **6**, 85495–85514.

49 C. Ribeiro, V. Sencadas, J. L. G. Ribelles and S. Lanceros-Méndez, *Soft Mater.*, 2010, **8**, 274–287.

50 D. M. Correia, C. Ribeiro, J. C. C. Ferreira, G. Botelho, J. L. G. Ribelles, S. Lanceros-Méndez and V. Sencadas, *Polym. Eng. Sci.*, 2014, **54**, 1608–1617.

51 S. Gee, B. Johnson and A. L. Smith, *J. Membr. Sci.*, 2018, **563**, 804–812.

52 R. Wang, Y. Liu, B. Li, B. S. Hsiao and B. Chu, *J. Membr. Sci.*, 2012, **392–393**, 167–174.

53 T. Mazoochi, M. Hamadanian, M. Ahmadi and V. Jabbari, *Int. J. Ind. Chem.*, 2012, **3**, 2.

54 S. De Vrieze, T. Van Camp, A. Nelvig, B. Hagström, P. Westbroek and K. De Clerck, *J. Mater. Sci.*, 2009, **44**, 1357–1362.

55 M. Essalhi and M. Khayet, *J. Membr. Sci.*, 2013, **433**, 167–179.

56 G. Kim, Y.-S. Cho and W. D. Kim, *Eur. Polym. J.*, 2006, **42**, 2031–2038.

57 I. G. Loscertales, A. Barrero, M. Márquez, R. Spretz, R. Velarde-Ortiz and G. Larsen, *J. Am. Chem. Soc.*, 2004, **126**, 5376–5377.

58 S. M. Moghadam, Y. Dong, S. Barbhuiya, L. Guo, D. Liu, R. Umer, X. Qi and Y. Tang, *Electrospinning: Current Status and Future Trends*, 2016, pp. 89–154, DOI: 10.1007/978-3-319-39715-3_4.
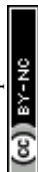
59 B. Lu, Y. Wang, Y. Liu, H. Duan, J. Zhou, Z. Zhang, Y. Wang, X. Li, W. Wang, W. Lan and E. Xie, *Small*, 2010, **6**, 1612–1616.

60 W. S. Khan, R. Asmatulu, M. Ceylan and A. Jabbarnia, *Fibers Polym.*, 2013, **14**, 1235–1247.

61 L. Persano, A. Camposeo, C. Tekmen and D. Pisignano, *Macromol. Mater. Eng.*, 2013, **298**, 504–520.

62 B. Ding, X. Wang and J. Yu, *Electrospinning: Nanofabrication and Applications*, Elsevier Science, 2018.

63 J. A. Matthews, G. E. Wnek, D. G. Simpson and G. L. Bowlin, *Biomacromolecules*, 2002, **3**, 232–238.

64 P. Katta, M. Alessandro, R. D. Ramsier and G. G. Chase, *Nano Lett.*, 2004, **4**, 2215–2218.

65 B. Sundaray, V. Subramanian, T. S. Natarajan, R.-Z. Xiang, C.-C. Chang and W.-S. Fann, *Appl. Phys. Lett.*, 2004, **84**, 1222–1224.

66 W. E. Teo, M. Kotaki, X. M. Mo and S. Ramakrishna, *Nanotechnology*, 2005, **16**, 918–924.

67 N. Bhattarai, D. Edmondson, O. Veiseh, F. A. Matsen and M. Zhang, *Biomaterials*, 2005, **26**, 6176–6184.

68 C. Y. Xu, R. Inai, M. Kotaki and S. Ramakrishna, *Biomaterials*, 2004, **25**, 877–886.

69 J. Wu and Y. Hong, *Bioactive Materials*, 2016, **1**, 56–64.

70 M.-S. Khil, S. R. Bhattarai, H.-Y. Kim, S.-Z. Kim and K.-H. Lee, *J. Biomed. Mater. Res., Part B*, 2005, **72**, 117–124.

71 D. Li, Y. Wang and Y. Xia, *Nano Lett.*, 2003, **3**, 1167–1171.

72 C.-Y. Pan, G.-R. Xu, K. Xu, H.-L. Zhao, Y.-Q. Wu, H.-C. Su, J.-M. Xu and R. Das, *Sep. Purif. Technol.*, 2019, **221**, 44–63.

73 T. Kawasaki and M. Yoshikawa, *Desalin. Water Treat.*, 2013, **51**, 5080–5088.

74 M. Lee, S. An, S. Latthe, C. Lee, S. Hong and S. Yoon, *ACS Appl. Mater. Interfaces*, 2013, **5**, 10597–10604.

75 L. Li, R. Hashaikeh and H. A. Arafat, *J. Membr. Sci.*, 2013, **436**, 57–67.

76 Y. Liu, R. Wang, H. Ma, B. Hsiao and B. Chu, *Polymer*, 2013, **54**, 548–556.

77 J.-G. Gai and X.-L. Gong, *J. Mater. Chem. A*, 2014, **2**, 425–429.

78 E. Ghasemi, H. Ziyadi, A. M. Afshar and M. Sillanpää, *Chem. Eng. J.*, 2015, **264**, 146–151.

79 H. Hallaji, A. R. Keshtkar and M. A. Moosavian, *J. Taiwan Inst. Chem. Eng.*, 2015, **46**, 109–118.

80 A. Mahapatra, B. G. Mishra and G. Hota, *Ind. Eng. Chem. Res.*, 2013, **52**, 1554–1561.

81 M. J. Nalbandian, K. E. Greenstein, D. Shuai, M. Zhang, Y.-H. Choa, G. F. Parkin, N. V. Myung and D. M. Cwiertny, *Environ. Sci. Technol.*, 2015, **49**, 1654–1663.

82 M. Obaid, N. Barakat, O. Fadali, M. Motlak, A. Almajid and A. Khalil, *Chem. Eng. J.*, 2015, **259**, 449–456.

83 M. Tian, C. Qiu, Y. Liao, S. R. Chou and R. Wang, *Sep. Purif. Technol.*, 2013, **118**, 727–736.

84 E. L. Tian, H. Zhou, Y. W. Ren, Z. a. mirza, X. Z. Wang and S. W. Xiong, *Desalination*, 2014, **347**, 207–214.

85 H. You, X. Li, Y. Yang, B. Wang, Z. Li, X. Wang, M. Zhu and B. Hsiao, *Sep. Purif. Technol.*, 2013, **108**, 143–151.

86 L. Huang, J. Arena, S. Manickam, X. Jiang, B. Willis and J. McCutcheon, *J. Membr. Sci.*, 2014, **460**, 241–249.

87 I. Tlili and T. A. Alkanhal, *J. Water Reuse Desalin.*, 2019, **9**, 232–248.

88 S. M. Seyed Shahabadi, S. Mousavi and D. Bastani, *J. Taiwan Inst. Chem. Eng.*, 2016, **59**, 474–483.

89 M. Khamforoush, O. Pirouzram and T. Hatami, *Desalination*, 2015, **359**, 14–21.

90 A. Almasian, M. Olya and N. M. Mahmoodi, *J. Taiwan Inst. Chem. Eng.*, 2015, **49**, 119–128.

91 G. Hong, L. Shen, M. Wang, Y. Yang, X. Wang, M. Zhu and B. Hsiao, *Chem. Eng. J.*, 2014, **244**, 307–316.

92 S. Anitha, B. Balusamy, D. Thiruvadigal, C. Gopalakrishnan and T. Natarajan, *Carbohydr. Polym.*, 2012, **87**, 1065–1072.

93 W. Huang, Y. Wang, C. Chen, J. L. M. Law, M. Houghton and L. Chen, *Carbohydr. Polym.*, 2016, **143**, 9–17.

94 A. Abdelsamad, B. Kwankhao, T. Gad-Allah, A. Khalil, M. Badawy, T. Bahners and M. Ulbricht, *Desalin. Water Treat.*, 2017, **86**, 89.

95 J. Dolina, T. Jiříček and T. Lederer, *Ind. Eng. Chem. Res.*, 2013, **52**, 13971–13978.

96 C. Feng, K. Khulbe, T. Matsuura, S. Tabe and A. Ismail, *Sep. Purif. Technol.*, 2013, **102**, 118–135.

97 T. He, W. Zhou, A. Bahi, H. Yang and F. Ko, *Chem. Eng. J.*, 2014, **252**, 327–336.

98 L. Huang, J. T. Arena and J. R. McCutcheon, *J. Membr. Sci.*, 2016, **499**, 352–360.

99 S. Homaeigohar, T. Dai and M. Elbahri, *J. Colloid Interface Sci.*, 2013, **406**, 86–93.

100 L. Huang and J. R. McCutcheon, *J. Membr. Sci.*, 2014, **457**, 162–169.

101 M. A. Kanjwal, N. A. M. Barakat and I. S. Chronakis, *Ceram. Int.*, 2015, **41**, 9615–9621.

102 X. Li, N. Wang, G. Fan, J. Yu, J. Gao, G. Sun and B. Ding, *J. Colloid Interface Sci.*, 2015, **439**, 12–20.

103 L. Li, Y. Li and C. Yang, *Carbohydr. Polym.*, 2016, **140**, 299–307.

104 N. Horzum, E. Boyacı, A. E. Eroğlu, T. Shahwan and M. M. Demir, *Biomacromolecules*, 2010, **11**, 3301–3308.

105 M. Hilal Elhousseini, T. Isık, Ö. Kap, F. Verpoort and N. Horzum, *Appl. Surf. Sci.*, 2020, **514**, 145939.

106 Y. Liu, R. Wang, H. Ma, B. S. Hsiao and B. Chu, *Polymer*, 2013, **54**, 548–556.

107 J. Yu, Y.-G. Kim, D. Y. Kim, S. Lee, H.-I. Joh and S. M. Jo, *Macromol. Res.*, 2015, **23**, 601–606.

108 J. Bae, I. Baek and H. Choi, *Water Res.*, 2016, **105**, 406–412.

109 R. K. Sadasivam, S. Mohiyuddin and G. Packirisamy, *ACS Omega*, 2017, **2**, 6556–6569.

110 R. Wang, S. Guan, A. Sato, X. Wang, Z. Wang, R. Yang, B. S. Hsiao and B. Chu, *J. Membr. Sci.*, 2013, **446**, 376–382.

111 Y. Liu, P. Cheng, Q. Guo, N. Liu, Y. Wan, W. Zhong, Z. Lu, K. Liu, G. Sun and D. Wang, *Composites Communications*, 2020, **21**, 100379.

112 L. Li, R. Hashaikeh and H. Arafat, *Development of eco-efficient micro-porous membranes via electrospinning and annealing of poly (lactic acid)*, 2013.

113 L. A. Goetz, B. Jalvo, R. Rosal and A. P. Mathew, *J. Membr. Sci.*, 2016, **510**, 238–248.

114 M. Alsehli, J.-K. Choi and M. Aljuhan, *Sol. Energy*, 2017, **153**, 348–359.

115 P. Guo, T. Li, P. Li, Y. Zhai and J. Li, *Desalination*, 2020, **473**, 114195.

116 J. Ravi, M. H. D. Othman, T. Matsuura, M. Ro'il Bilad, T. H. El-badawy, F. Aziz, A. F. Ismail, M. A. Rahman and J. Jaafar, *Desalination*, 2020, **490**, 114530.

117 S. F. Anis, R. Hashaikeh and N. Hilal, *Desalination*, 2019, **452**, 159–195.

118 N. Akther, S. Phuntsho, Y. Chen, N. Ghaffour and H. K. Shon, *J. Membr. Sci.*, 2019, **584**, 20–45.

119 S. Homaeigohar and M. Elbahri, *NPG Asia Mater.*, 2017, **9**, e427.

120 L. D. Tijing, Y. C. Woo, J.-S. Choi, S. Lee, S.-H. Kim and H. K. Shon, *J. Membr. Sci.*, 2015, **475**, 215–244.

121 S. Lin, N. Y. Yip and M. Elimelech, *J. Membr. Sci.*, 2014, **453**, 498–515.

122 K.-K. Yan, L. Jiao, S. Lin, X. Ji, Y. Lu and L. Zhang, *Desalination*, 2018, **437**, 26–33.

123 M. M. A. Shirazi, A. Kargari, D. Bastani and L. Fatehi, *Desalin. Water Treat.*, 2014, **52**, 2372–2381.

124 Y. C. Woo, L. D. Tijing, W.-G. Shim, J.-S. Choi, S.-H. Kim, T. He, E. Drioli and H. K. Shon, *J. Membr. Sci.*, 2016, **520**, 99–110.

125 E. Drioli, A. Ali and F. Macedonio, *Desalination*, 2015, **356**, 56–84.

126 A. A. Kiss and O. M. Kattan Readi, *J. Chem. Technol. Biotechnol.*, 2018, **93**, 2047–2055.

127 Y. Liao, C.-H. Loh, M. Tian, R. Wang and A. G. Fane, *Prog. Polym. Sci.*, 2018, **77**, 69–94.

128 L. D. Tijing, J.-S. Choi, S. Lee, S.-H. Kim and H. K. Shon, *J. Membr. Sci.*, 2014, **453**, 435–462.

129 M. Essalhi and M. Khayet, *J. Membr. Sci.*, 2014, **454**, 133–143.

130 M. Yao, Y. C. Woo, L. Tijing, W.-G. Shim, J.-S. Choi, S.-H. Kim and H. K. Shon, *Desalination*, 2016, **378**, 80–91.

131 B. Lalia, E. Guillén-Burrieza, H. Arafat and R. Hashaikeh, *Desalination*, 2014, **332**, 134–141.

132 E.-J. Lee, A. K. An, P. Hadi, S. Lee, Y. C. Woo and H. K. Shon, *J. Membr. Sci.*, 2017, **524**, 712–720.

133 Z.-Q. Dong, X.-h. Ma, Z.-L. Xu, W.-T. You and F.-b. Li, *Desalination*, 2014, **347**, 175–183.

134 Y. Liao, R. Wang and A. G. Fane, *J. Membr. Sci.*, 2013, **440**, 77–87.

135 X. An, Z. Liu and Y. Hu, *Desalination*, 2018, **432**, 23–31.

136 Y. Liao, C. H. Loh, R. Wang and T. Fane, *ACS Appl. Mater. Interfaces*, 2014, **6**, 16035–16048.

137 Y. Liao, R. Wang and A. G. Fane, *Environ. Sci. Technol.*, 2014, **48**, 6335–6341.

138 E.-J. Lee, A. K. An, T. He, Y. C. Woo and H. K. Shon, *J. Membr. Sci.*, 2016, **520**, 145–154.

139 Z.-Q. Dong, B.-J. Wang, X.-h. Ma, Y.-M. Wei and Z.-L. Xu, *ACS Appl. Mater. Interfaces*, 2015, **7**, 22652–22659.

140 F. Yang, J. E. Efome, D. Rana, T. Matsuura and C. Lan, *ACS Appl. Mater. Interfaces*, 2018, **10**, 11251–11260.

141 A. Kyoungjin An, E.-J. Lee, J. Guo, S. Jeong, J.-G. Lee and N. Ghaffour, *Sci. Rep.*, 2017, **7**, 41562.

142 F. Guo, A. Servi, A. Liu, K. K. Gleason and G. C. Rutledge, *ACS Appl. Mater. Interfaces*, 2015, **7**, 8225–8232.

143 Y. Chul Woo, Y. Chen, L. D. Tijing, S. Phuntsho, T. He, J.-S. Choi, S.-H. Kim and H. Kyong Shon, *J. Membr. Sci.*, 2017, **529**, 234–242.

144 Y. C. Woo, L. D. Tijing, M. J. Park, M. Yao, J.-S. Choi, S. Lee, S.-H. Kim, K.-J. An and H. K. Shon, *Desalination*, 2017, **403**, 187–198.

145 L. F. Greenlee, D. F. Lawler, B. D. Freeman, B. Marrot and P. Moulin, *Water Res.*, 2009, **43**, 2317–2348.

146 M. Asadollahi, D. Bastani and S. A. Musavi, *Desalination*, 2017, **420**, 330–383.

147 S. Subramanian and R. Seeram, *Desalination*, 2013, **308**, 198–208.

148 A. K. Ghosh and E. M. V. Hoek, *J. Membr. Sci.*, 2009, **336**, 140–148.

149 X. Wang, H. Ma, B. Chu and B. S. Hsiao, *Desalination*, 2017, **420**, 91–98.

150 S. Kim, D. E. Heath and S. E. Kentish, *ACS Appl. Mater. Interfaces*, 2020, **12**, 44720–44730.

151 M. Amjad, J. Gardy, A. Hassanpour and D. Wen, *Appl. Energy*, 2018, **230**, 220–231.

152 M. Tian, C. Qiu, Y. Liao, S. Chou and R. Wang, *Sep. Purif. Technol.*, 2013, **118**, 727–736.

153 L. A. Hoover, J. D. Schiffman and M. Elimelech, *Desalination*, 2013, **308**, 73–81.

154 L. Huang and J. R. McCutcheon, *J. Membr. Sci.*, 2015, **483**, 25–33.

155 M. Tian, R. Wang, K. Goh, Y. Liao and A. G. Fane, *J. Membr. Sci.*, 2015, **486**, 151–160.

156 J. M. C. Puguan, H.-S. Kim, K.-J. Lee and H. Kim, *Desalination*, 2014, **336**, 24–31.

157 E. L. Tian, H. Zhou, Y. W. Ren, Z. a. mirza, X. Z. Wang and S. W. Xiong, *Desalination*, 2014, **347**, 207–214.

158 J. Cui, F. Li, Y. Wang, Q. Zhang, W. Ma and C. Huang, *Sep. Purif. Technol.*, 2020, **250**, 117116.

159 Y. Si, T. Ren, B. Ding, J. Yu and G. Sun, *J. Mater. Chem.*, 2012, **22**, 4619–4622.

160 Q. Wang, J. Ju, Y. Tan, L. Hao, Y. Ma, Y. Wu, H. Zhang, Y. Xia and K. Sui, *Carbohydr. Polym.*, 2019, **205**, 125–134.

161 R. Zhao, Y. Wang, X. Li, B. Sun and C. Wang, *ACS Appl. Mater. Interfaces*, 2015, **7**, 26649–26657.

162 R. Al-Qassar Bani Al-Marjeh, Y. Atassi, N. Mohammad and Y. Badour, *Environ. Sci. Pollut. Res.*, 2019, **26**, 37282–37295.

163 W. Jang, J. Yun, Y. Seo, H. Byun, J. Hou and J.-H. Kim, *Polymers*, 2020, **12**, 2009.

164 R. Sharma, N. Singh, A. Gupta, S. Tiwari, S. K. Tiwari and S. R. Dhakate, *J. Mater. Chem. A*, 2014, **2**, 16669–16677.

165 Q. Feng, D. Wu, Y. Zhao, A. Wei, Q. Wei and H. Fong, *J. Hazard. Mater.*, 2018, **344**, 819–828.

166 Sapna, R. Sharma and D. Kumar, in *Nanoscale Materials in Water Purification*, ed. S. Thomas, D. Pasquini, S.-Y. Leu and D. A. Gopakumar, Elsevier, 2019, pp. 799–814, DOI: 10.1016/B978-0-12-813926-4.00037-9.

167 L.-L. Min, Z.-H. Yuan, L.-B. Zhong, Q. Liu, R.-X. Wu and Y.-M. Zheng, *Chem. Eng. J.*, 2015, **267**, 132–141.

168 D. Yang, L. Li, B. Chen, S. Shi, J. Nie and G. Ma, *Polymer*, 2019, **163**, 74–85.

169 M. Aliabadi, M. Irani, J. Ismaeili and S. Najafzadeh, *J. Taiwan Inst. Chem. Eng.*, 2014, **45**, 518–526.

170 I. Lakhdhar, P. Mangin and B. Chabot, *Journal of Water Process Engineering*, 2015, **7**, 295–305.

171 A. R. Keshtkar, M. Irani and M. A. Moosavian, *J. Radioanal. Nucl. Chem.*, 2013, **295**, 563–571.

172 S. Zhou, F. Liu, Q. Zhang, B.-Y. Chen, C.-J. Lin and C.-T. Chang, *J. Nanosci. Nanotechnol.*, 2015, **15**, 5823–5832.

173 J.-J. Wu, H.-W. Lee, J.-H. You, Y.-C. Kau and S.-J. Liu, *J. Colloid Interface Sci.*, 2014, **420**, 145–151.

174 S. Yang, Y. Si, Q. Fu, F. Hong, J. Yu, S. S. Al-Deyab, M. El-Newehy and B. Ding, *Nanoscale*, 2014, **6**, 12445–12449.

175 Z. Jiang, L. D. Tijing, A. Amarjargal, C. H. Park, K.-J. An, H. K. Shon and C. S. Kim, *Composites, Part B*, 2015, **77**, 311–318.

176 X. Tang, Y. Si, J. Ge, B. Ding, L. Liu, G. Zheng, W. Luo and J. Yu, *Nanoscale*, 2013, **5**, 11657–11664.

177 F. Ejaz Ahmed, B. S. Lalia, N. Hilal and R. Hashaikeh, *Desalination*, 2014, **344**, 48–54.

178 A. Raza, B. Ding, G. Zainab, M. El-Newehy, S. S. Al-Deyab and J. Yu, *J. Mater. Chem. A*, 2014, **2**, 10137–10145.

179 P.-Y. Chen and S.-H. Tung, *Macromolecules*, 2017, **50**, 2528–2534.

180 J.-J. Li, Y.-N. Zhou and Z.-H. Luo, *ACS Appl. Mater. Interfaces*, 2015, **7**, 19643–19650.

181 W. Ma, M. Zhang, Z. Liu, M. Kang, C. Huang and G. Fu, *J. Membr. Sci.*, 2019, **570–571**, 303–313.

182 Y. Yi, H. Tu, X. Zhou, R. Liu, Y. Wu, D. Li, Q. Wang, X. Shi and H. Deng, *J. Hazard. Mater.*, 2019, **371**, 165–174.

183 Z. Zhu, W. Wang, D. Qi, Y. Luo, Y. Liu, Y. Xu, F. Cui, C. Wang and X. Chen, *Adv. Mater.*, 2018, **30**, 1801870.